Analysis of the metabolic pathways affected by hot-humid or dry climate based on fecal metabolomics coupled with serum metabolic changes in broiler chickens

Ying Zhou,* Huchuan Liu,† and Minhong Zhang*,[1]

*State Key Laboratory of Animal Nutrition, Institute of Animal Science, Chinese Academy of Agricultural Science, Beijing 100193, PR China; and †Department of Technology Management, Qingdao Research Institute of Husbanary and Veterinary, Qingdao 266100, PR China

ABSTRACT Air temperature and relative humidity (**RH**) are 2 important climatic elements that affect animal welfare and health. The prevailing hot and humid or dry climate is one of the major constraints for optimum poultry production, especially in the tropics and subtropical regions. Many studies have suggested that exposure to hot-humid or dry climate is associated with a high risk of metabolic imbalance; however, the underlying metabolic changes caused by low or high RH climate is not yet well understood. Therefore, we used a comprehensive ultra-high-performance liquid chromatography coupled with quadrupole time-of-flight mass spectrometry–based metabolic profiling of fecal samples to explore the effects of hot-humid and dry climate on metabolic pathways in broilers. A total of 180 twenty-eight-day-old Arbor Acres broilers were randomly allocated to 3 treatments, each containing 6 replicates of 10 birds per treatment, using a completely randomized design. Birds were reared at 35, 60, or 85% RH at 32°C (temperature increased by 3°C every 3 d from 20°C to 32°C within 15 d: 20°C, 23°C, 26°C, 29°C, 32°C) for 15 d. Results showed that significant changes in the levels of 36 metabolites were detected. Evidence of changes in gluconeogenesis associated to pyruvate metabolism, galactose metabolism, and ABC transporter was observed. In addition, hot-humid and dry stress also affected the protein translation process caused by aminoacyl-tRNA biosynthesis, which may be associated with protein synthesis and hormone secretion disorders. Furthermore, we observed significant changes in primary bile acid biosynthesis and taurine and hypotaurine metabolism, which indicated that fat synthesis was affected. We also observed significant changes in arginine and proline metabolism and histidine metabolism, which were associated with skin vasodilation and blood flow. These results provide biochemical insights into metabolic changes due to hot-humid or dry climate.

Key words: broiler, hot humid or dry climate, metabolic pathway, fecal metabolomics, serum metabolic change

2020 Poultry Science 99:5526–5546
https://doi.org/10.1016/j.psj.2020.07.039

INTRODUCTION

Air temperature and humidity are 2 important climatic elements that affect animal welfare and health. There is always a relationship between temperature and humidity and its effect on the body (Tseliou et al. 2010). Over the past 2 decades, the global animal production has increased, especially in tropical and subtropical areas, and more than 50% of total world meat originates from tropical and subtropical areas (FAO, 2010). However, the prevailing hot and humid or dry climate is one of the major constraints for optimum poultry production in the tropics and subtropical regions. High ambient temperature and high relative humidity (**RH**) or low RH occurring during the hot-humid or dry season have been shown to cause heat stress in broilers (Ayo et al., 2011; Minka and Ayo, 2012). The fast growing commercial broiler chickens are particularly susceptible to heat stress that induces metabolic disorder (Olubodun et al., 2015; Yousaf et al., 2018, 2019). In addition, global warming will further accentuate heat stress–related problems. Therefore, elucidating the metabolic route is critical in hot-humid or dry climate, especially for providing a chemical route for easing the adverse influence of RH because RH is seldom directly measured or managed and is not possible to control as narrowly as temperature (Dawkins et al. 2004).

© 2020 Published by Elsevier Inc. on behalf of Poultry Science Association Inc. This is an open access article under the CC BY-NC-ND license (http://creativecommons.org/licenses/by-nc-nd/4.0/).

Received April 3, 2020.
Accepted July 6, 2020.

[1]Corresponding author: zmh66@126.com

A considerable body of evidence suggests that both high and low RH at high temperatures decreased the growth performance of broilers (Milligan and Winn, 1964; Adams and Rogler, 1968; Reece et al., 1972; Misson, 1976; Yahav et al., 1995, Yahav, 2000; Zhou et al., 2017, 2019a, 2019b). At high temperatures, heat production decreases while heat dissipation increases (Lin et al., 2005). The main route of heat dissipation for birds under hot environment is evaporation. The amount of evaporated heat loss depends on air humidity and is suppressed when humidity rises (Chwalibog and Eggum, 1989; Nichelmann et al., 1991; Lin et al., 2005). Our preliminary research suggests that the decreased growth rate is associated with energy imbalance, as increased glucose consumption and reduced mitochondrial adenosine diphosphate (**ATP**) production (Zhou et al., 2019b). However, the exact metabolic route underlying the decreased growth and suppressed heat dissipation related to RH stress at high temperatures still need to be elucidated.

Metabolomics is becoming an increasingly used tool for exhaustive studies of all metabolites present in an organism (Lau et al., 2015). It is known that external perturbations imposed on organisms can produce changes in their metabolites. These perturbations can be pathophysiological stimuli, environmental changes, nutritional stresses, and genetic modifications (Nicholson et al., 1999; Navarro-Reig et al., 2015). Therefore, metabolomics can be used to identify novel and potential metabolite markers and to explore molecular mechanisms and the response of metabolic pathways to different perturbations. Metabolomics is a novel technology with great potential for environmental changes research and provides a unique perspective on hot-humid or dry climate–induced changes in cellular metabolism (Booth et al., 2011).

The fast growing nature of commercial broiler chickens prompted us to investigate different metabolic pathways after hot-humid or dry stress. Here, we assume that the metabolite profiles are associated with hot-humid or dry climate–induced pathophysiological processes. Therefore, to execute a large-scale detection of the metabolite features in fecal samples, untargeted fecal metabolomics based on ultra-high-performance liquid chromatography coupled with quadrupole time-of-flight mass spectrometry (**UHPLC-Q-TOF/MS**) with high-resolution, high-throughput, and highly sensitive technology was performed in this research (Plumb et al., 2005; van der Greef et al., 2013). An untargeted metabolomics work flow that acquires MS and MS/MS data sequentially was designed (Figure 5). Quantitative information is extracted from MS data using XCMS Online, and metabolite features are simultaneously characterized by matching the MS/MS data to the METLIN database (Benton et al., 2015). With the approach of metabolomics analysis, the versatile effects of hot-humid or dry climate on different metabolic pathways in fecal samples and more details on the mechanisms of action after hot-humid or dry stress could be observed.

MATERIALS AND METHODS

Experimental Design, Animals, and Management

All experimental procedures involving the use of animals were approved by the the Animal Management Committee (in charge of animal welfare issues) of the Institute of Animal Science, Chinese Academy of Agricultural Sciences (IAS-CAAS, Beijing, China) and performed in accordance with the guidelines. Ethical approval on animal survival was given by the Animal Ethics Committee of IAS-CAAS (certification no.: IAS-2019-42).

One-day-old broiler chicks (Arbor Acres broilers) were reared in environmental chambers under continuous light for up to 3 wk. At 21 d of age, 180 broilers with a similar body weight (1.22 ± 0.03 kg) were randomly assigned to one of 3 treatments (35, 60, or 85% RH with an accuracy of ±7%), including 6 replicate cages with 10 birds per cage. Birds were kept at 20°C and 60% RH for 1 wk to adapt to the chamber environment. The temperature was then gradually increased by 3°C at 10:00 pm every 3 d from 20°C to 32°C (with an accuracy of ±1°C) over the course of 15 d. The experiment period ends at the 42 d of age. The experimental diet was designed according to the National Research Council (NRC, 1994) guidelines. The composition and nutrient levels of the basal diets were shown in Table 1. All chicks were exposed to 24 h of constant light photoperiod during the entire experimental period. Feed and tap water were available ad libitum. Dead birds were recorded daily, and chick weight and feed intake per cage were measured weekly to calculate the average daily gain (**ADG**), average daily feed intake, feed conversion rate, and mortality.

Sample Collections and Preparations

After the temperature was raised to 32°C for 48 h, the skin temperature, rectal temperature, and respiratory rate were measured.

The fecal samples were collected at 10:00 am (48 h after the temperature was raised to 32°C). Then the fecal samples were immediately frozen in liquid nitrogen and then stored at −80°C for metabolomics analysis. To facilitate individual sampling and quantitative collection of all voided feces without handling the animal, we used a method similar to the one described by Touma et al. (2003). Briefly, every 10 broilers were housed individually in stainless steel wire cages (87 × 85 × 40 cm), which were placed in environment chambers of the same size. All excreta dropped through the bars of the steel wire cage and could be easily collected from the floor of the lower cage, which was completely covered

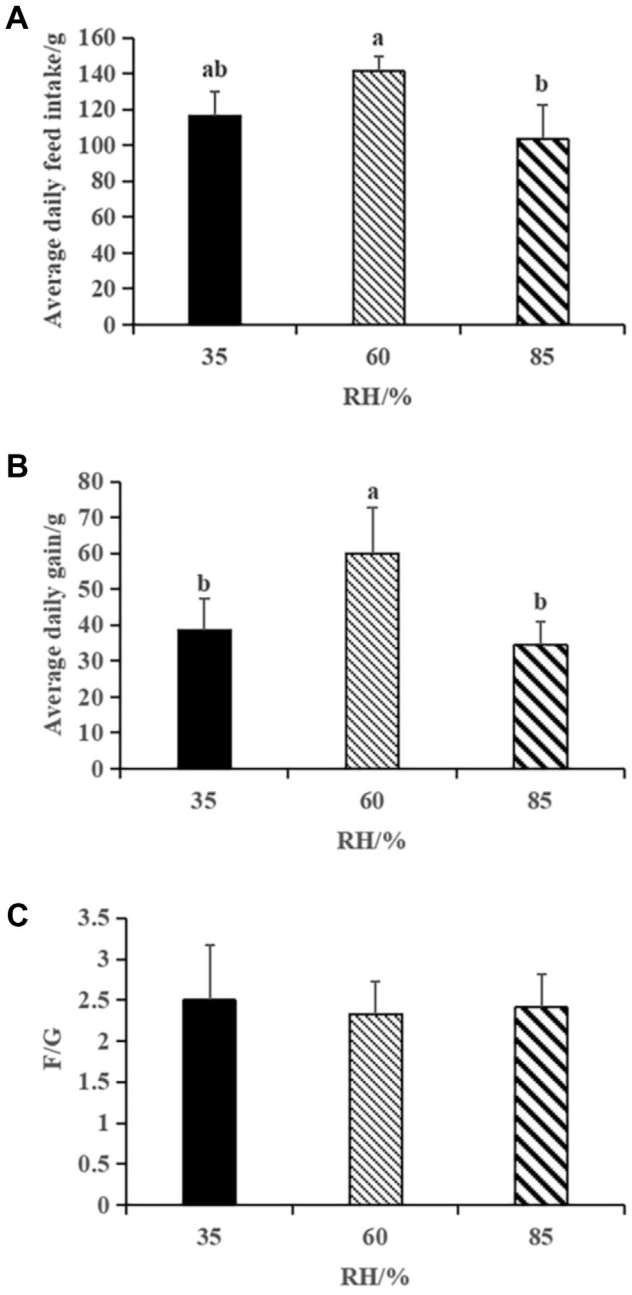

Figure 1. Effects of hot-humid, mid, or dry stress on growth performance of broilers: (A) average daily feed intake (ADFI), (B) average daily gain (ADG), (C) feed intake:gain (F/G). Different lowercase letters within the same time points indicate significant differences among the 3 treatments ($P < 0.05$). Abbreviation: RH, relative humidity.

with 1 × 1-m black garbage bags. During each sampling, the black garbage bags were renewed.

At 42 d of age, birds were individually weighed after a 12-h fast, and 6 birds were chosen from each chamber (one bird per cage). Blood samples were collected into tubes without anticoagulant and centrifuged at 1,400 × *g* for 10 min at 4°C for analysis of blood glucose, urea, triiodothyronine (**T_3**), thyroxine (**T_4**), alkaline phosphatase (**AKP**), creatine kinase (**CK**), and corticosterone (**CORT**). Birds were then sacrificed by cervical dislocation. The hypothalamus was taken and frozen at −80°C for analysis of heat shock protein 70 (**HSP70**). The right breast muscle was removed and frozen at −80°C for analysis of glycogen levels and avian uncoupling protein (**av UCP**) mRNA expression. Liver samples were also taken and frozen at −80°C for analysis of glycogen levels.

Measurements of Respiratory Rate, Core Body Temperature, Skin Temperature

The specific method of skin temperature measurement is by using the infrared thermal imager FLIR E4 (thermal resolution 0.07°C, accuracy ±2%) to shoot the side of the broiler head vertically, the shooting distance is 0.5 m, shooting once every 3 min, continuous shoot 1 h, and take 20 infrared photos per chicken. Through the FLIR Tools software analysis, the skin temperature of the leg, flipper, earlobe, comb, and eyelids in each photograph was measured, and the average value of 20 data of the same chicken was taken as the true skin temperature value. The method for determining the core temperature involves randomly selecting one chicken in each replicate of each group and inserting a digital thermometer (Model. JM 6200, resolution 0.01°C) with a 5-cm-long probe into the rectum almost, and recording the value after stabilization. The core body temperature was recorded every 5 s and for a total of 4 times, and the average value was taken. The respiratory rate was measured once every 10 min, and the number of breaths in broilers within 1 min was measured. A total of 6 breaths were collected, and the respiratory rate was the average of 6 breaths.

Determination of Glucose, Glycogen, and Urea

Glucose and urea concentrations in the blood, and glycogen levels in both the muscle and liver were determined using commercial assay kits (Nanjing Jiancheng Bioengineering Institute, Nanjing, China), according to the manufacturer's instructions.

Hormone Concentrations of Serum and Hypothalamus HSP70

T_3, T_4, AKP, CK, CORT, and HSP70 were measured by using commercial enzyme-linked immunosorbent assay (**ELISA**) kits specific for chicken (Nanjing Jiancheng Bioengineering Institute, Nanjing, China), according to the manufacturer's instructions.

RNA Extraction and Real-Time Polymerase Chain Reaction Assay

Av UCP expression (F:5-ATCGGGCTCT ACGACTCTGT-3, R:5-TGTGTCCTTGATGA GGTCGT-3, 327 bp) was determined using the quantitative real-time PCR. Total mRNA from the chest muscle was isolated using a TRIzol reagent (CW0581; ComWin Biotech, Beijing, China). Aliquots of the PCR products were sequenced (Takara Bio, Shiga, Japan) to verify authenticity. The quantification of

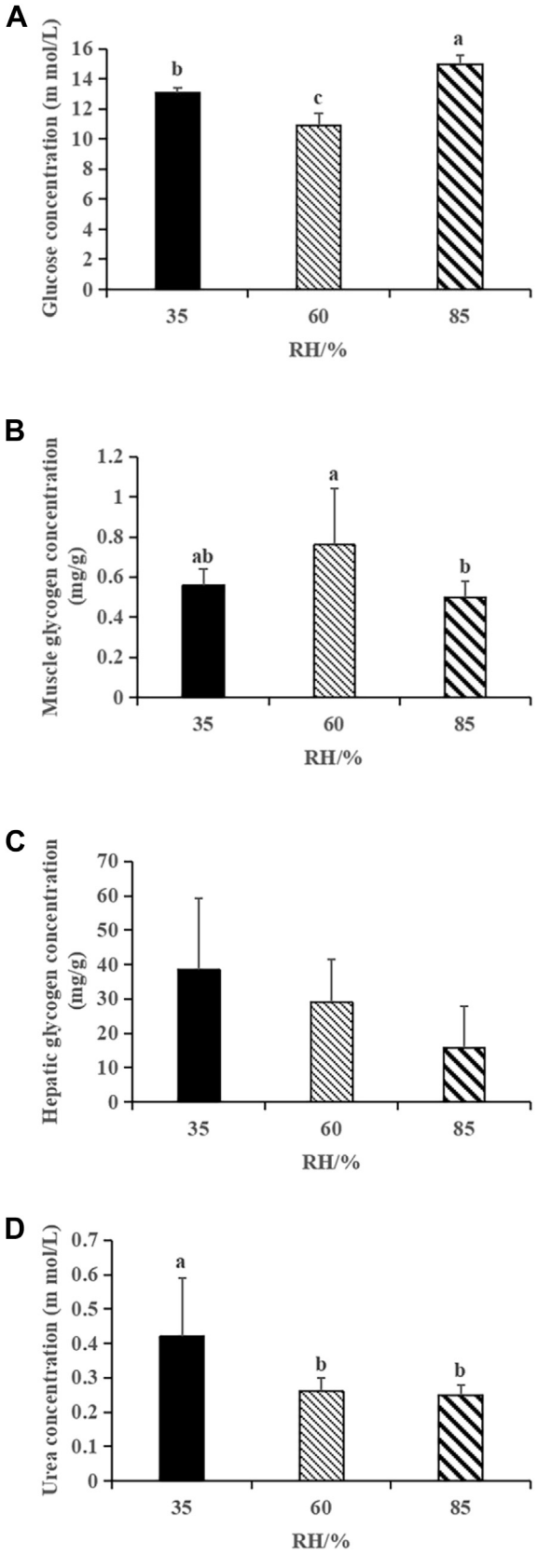

Figure 2. Effects of hot-humid, mid, or dry stress on the concentrations of blood glucose (A), muscle glycogen (B), liver glycogen (C), and blood urea (D) in broilers. Results are represented as the mean value ± SD of 6 sample birds per treatment (n = 6). Different lowercase letters within the same time points indicate significant differences among the 3 treatments ($P < 0.05$). Abbreviation: RH, relative humidity.

target gene expression was evaluated using the $2^{-\Delta\Delta Ct}$ method normalized to GAPDH (F:5-AACTTTG GCATTGTGGAGGG-3, R:5-ACGCTGGGATGATG TTCTGG-3, 130 bp).

Extraction of Fecal Samples and Quality Control Sample Preparation

Take about 10 g of frozen samples in a vacuum freeze drier fully lyophilized (LGJ-18; Beijing honored cologne instrument technology Co., Ltd.). Then take about approximately 25 mg of each chicken's lyophilized feces sample, add 1 mL of prechilled methanol/acetonitrile/water solution (2:2:1, v/v), vortex and mix, sonicate for 30 min/time, twice, and let stand at −20°C for 60 min. Centrifuge at 14,000 × *g* for 20 min at 4°C, take the supernatant, dry under vacuum, add 100 μL of acetonitrile aqueous solution (acetonitrile: water = 1:1, v/v) for redissolution during mass spectrometry, vortex, centrifuge at 14,000 × *g* at 4°C for 15 min, and take the supernatant for UHPLC-Q-TOF/MS analysis.

In parallel to the preparation of the test samples, we prepared a bulk quality control (**QC**) sample. The QC samples served 2 purposes. The first purpose was to act as a regular QC sample to monitor the LC-MS response in real time. Second, after the response had been characterized, the QC samples were used as standards of unknown composition to calibrate the data (Gika et al., 2007; Van Der Greef et al., 2007). The QC sample was made by mixing equal volumes (30 mL) from each of the samples being analyzed to create a pooled sample of sufficient volume to provide enough QC samples for the analytical run. Each aliquot of this sample was treated in the same way as the test samples.

UHPLC-MS Analysis

Metabolomics analysis was performed with an Agilent 1290 Infinity LC ultra-high-pressure liquid chromatograph (UHPLC) (Agilent, Palo Alto, CA) equipped with an electrospray ionization (ESI) source operating in positive and negative ion modes.

For HILIC separation, samples were analyzed using a 2.1 × 100-mm ACQUIY UPLC BEH 1.7-μm column (waters, Ireland). In both ESI positive and negative modes, the mobile phase contained A = 25-mmol/L ammonium acetate and 25-mmol/L ammonium hydroxide in water and B = acetonitrile. The gradient was 85% B for 1 min and was linearly reduced to 65% in 11 min; and then was reduced to 40% in 0.1 min and kept for 4 min; and then increased to 85% in 0.1 min, with a 5-min reequilibration period.

The ESI source conditions were set as follows: Ion Source Gas1 (Gas1) as 60, Ion Source Gas2 (Gas2) as 60, curtain gas (CUR) as 30, source temperature at 600°C, IonSpray Voltage Floating (ISVF) ±5,500 V. In MS-only acquisition, the instrument was set to

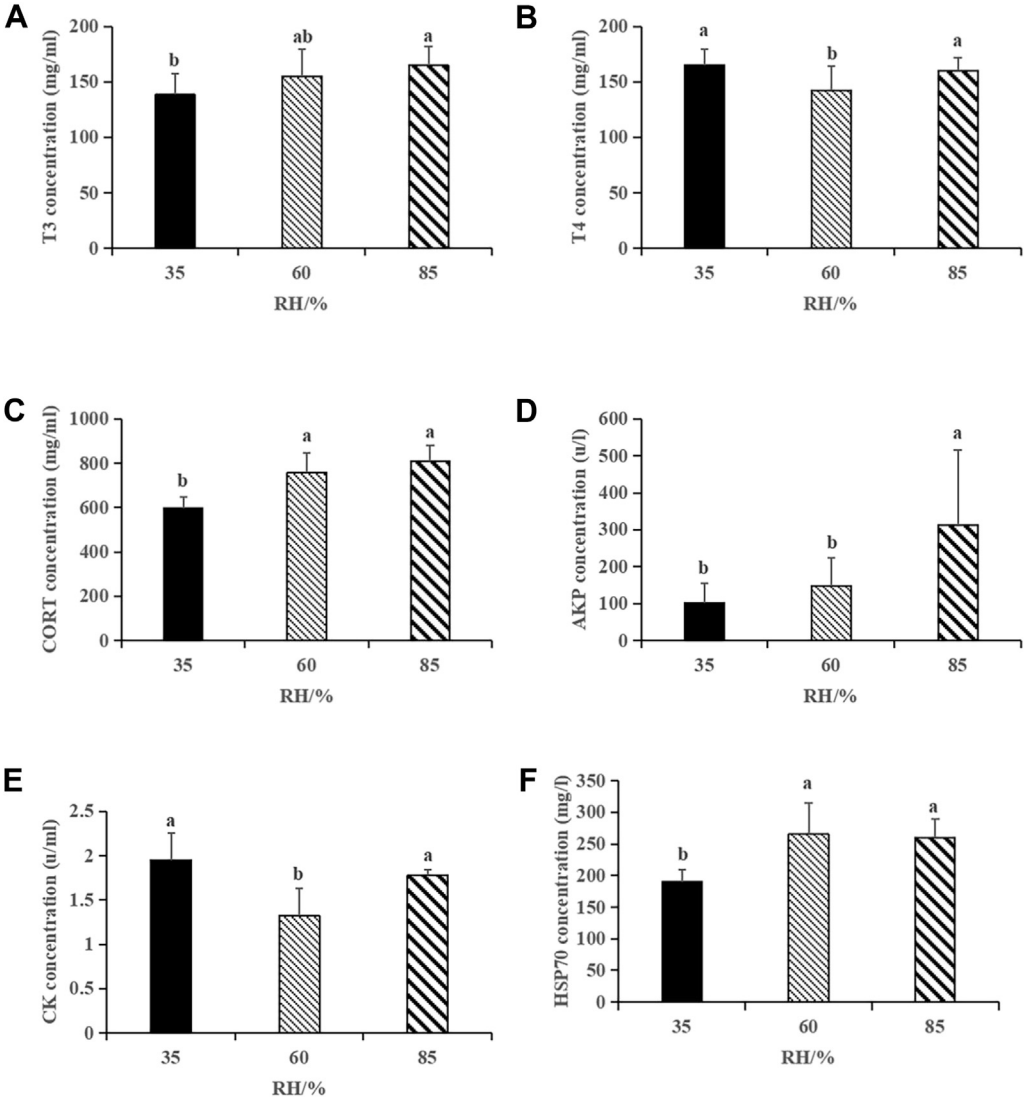

Figure 3. Effects of hot-humid, mid, or dry stress on the triiodothyronine T_3 (A), thyroxine T_4 (B), corticosterone (CORT) (C), alkaline phosphatase (AKP) (D), creatine kinase (CK) (E) in blood and heat shock protein (HSP70) (F) of broilers. Results are represented as the mean value ± SD of 6 sample birds per treatment (n = 6). Different lowercase letters within the same time points indicate significant differences among the 3 treatments ($P < 0.05$). Abbreviation: RH, relative humidity.

acquire over the m/z range 60 to 1,000 Da, and the accumulation time for TOF MS scan was set at 0.20 s/spectra. In auto MS/MS acquisition, the instrument was set to acquire over the m/z range 25 to 1,000 Da, and the accumulation time for product ion scan was set at 0.05 s/spectra. The product ion scan is acquired using information-dependent acquisition with the high-sensitivity mode selected. The collision energy was fixed at 35 V with ±15 eV. Declustering potential was set as ±60 V.

For RPLC separation, a 2.1 × 100-mm ACQUIY UPLC HSS T3 1.8-μm column (waters, Ireland) was used. In ESI-positive mode, the mobile phase contained A = water with 0.1% formic acid and B = acetonitrile with 0.1% formic acid, and in ESI negative mode, the mobile phase contained A = 0.5-mmol/L ammonium fluoride in water and B = acetonitrile. The gradient was 1% B for 1.5 min and was linearly increased to 99% in 11.5 min and kept for 3.5 min. Then it was reduced to 1% in 0.1 min, and 3.4 min of reequilibration period was used. The gradients were at a flow rate of 0.3 mL/min, and the column temperatures were kept constant at 25°C. A 2-μL aliquot of each sample was injected.

The ESI source conditions were set as follows: Ion Source Gas1 (Gas1) as 40, Ion Source Gas2 (Gas2) as 80, curtain gas (CUR) as 30, source temperature 650°C, IonSpray Voltage Floating (ISVF) 5,000 V in positive mode, and −4,000 V in negative mode. In MS-only acquisition, the instrument was set to acquire over the m/z range 60 to 1,000 Da, and the accumulation time for TOF MS scan was set at 0.20 s/spectra. In auto MS/MS acquisition, the instrument was set to acquire over the m/z range 25 to 1,000 Da, and the accumulation time for product ion scan was set at 0.05 s/spectra. The product ion scan is acquired using information-dependent acquisition with the high-sensitivity mode selected. The collision energy was fixed at 35 V with ±15 eV. Declustering potential was set as ±60 V.

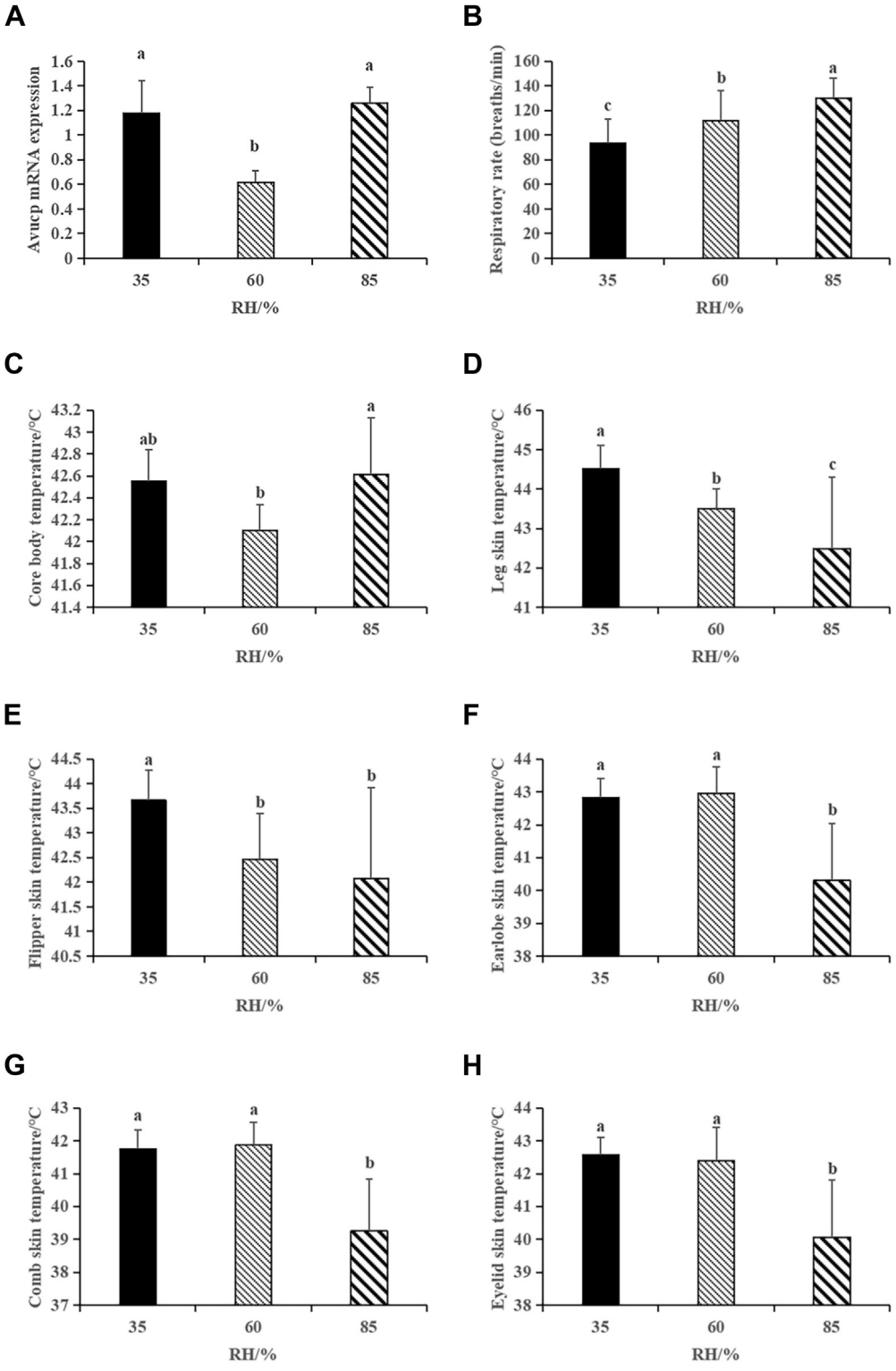

Figure 4. Effects of hot-humid, mid, or dry stress on the heat dissipation of broilers: (A) avian uncoupling protein (av UCP) expression, (B) respiratory rate, (C) core body temperature, (D) leg skin temperature, (E) flipper skin temperature, (F) earlobe skin temperature, (G) comb skin temperature, (H) eyelid skin temperature. Results are represented as the mean value ± SD of 6 sample birds per treatment (n = 6). Different lowercase letters within the same time points indicate significant differences among the 3 treatments ($P < 0.05$). Abbreviation: RH, relative humidity.

Data Deconvolution and Processing and Statistical Analysis

For XCMS, the raw data files were first converted into the mzML format via ProteoWizard, and subsequently the converted files were imported into the XCMS software for nonlinear alignment in the time domain, automatic integration, and extraction of the peak intensities, with default parameter settings. The data were subsequently processed using XCMS for peak alignment and data filtering. MetaboAnalyst 2.0 (http://www.metaboanalyst.ca) was used for the statistical analysis. Principle component analysis (PCA) and hierarchical clustering were performed for the unsupervised

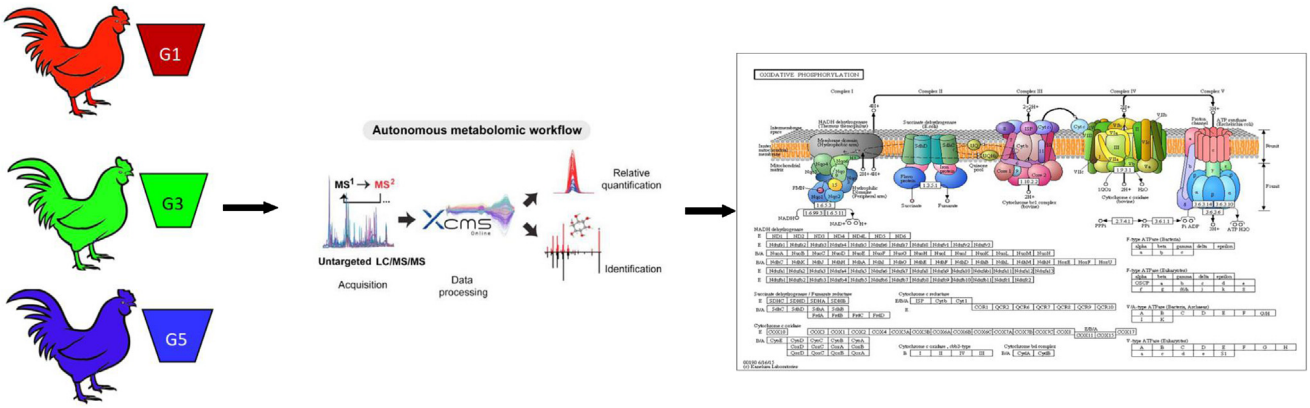

Figure 5. Schematic work flow of the experimental approach using autonomous untargeted metabolomics. Broilers (total 180 AA broilers: 3*6*10) were treated with changes in hot-humid, mid, or dry stress (G1: 35% RH at 32°C, G3: 60% RH at 32°C, G5: 85% RH at 32°C). Fecal samples were harvested for metabolomics profiling using untargeted metabolomics that acquires MS and MS/MS data sequentially. Quantitative information is extracted from the MS data using XCMS Online and identification followed by pathway correlation.

multivariate statistical analysis. Partial-least squares discrimination analysis (PLS-DA) was performed as a supervised method to identify the important variables with discriminative power. PLS-DA models were validated based on the multiple correlation coefficient (R2) and cross-validated R2 (Q2) in cross-validation and permutation tests by applying 2,000 iterations ($P > 0.001$). The significance of the biomarkers was ranked using the variable importance in projection (**VIP**) score (>1) from the PLS-DA model. For the univariate analysis, candidate-specific biomarkers were determined using single-dimensional statistical analysis for one-way ANOVA analysis. $P < 0.05$ was considered to be statistically significant.

Table 1. Composition and nutrient levels of the complete diets for broilers.

Item	1–3 wk	4–6 wk
Ingredients (%)		
Corn	53.36	56.51
Soybean meal	38.50	35.52
Soybean oil	4.10	4.50
NaCl	0.30	0.30
Limestone	1.15	1.00
$CaHPO_4$	2.01	1.78
DL-Met	0.22	0.11
Premix[1]	0.36[1]	0.28[2]
Total	100.00	100.00
Nutrient levels (%)[2]		
ME/(MJ kg^{-1})	12.46	12.73
CP	21.44	20.07
Ca	1.00	0.90
AP	0.45	0.40
Lys	1.17	1.00
Met	0.56	0.42
Met + Cys	0.91	0.78

[1]Premix provided per kg of diet for 1 to 3 wk: vitamin A, 12,500 IU; vitamin D_3, 3,750 IU; vitamin E, 16 IU; vitamin K_3, 2.0 mg; vitamin B_1, 2.5 mg; vitamin B_2, 8 mg; vitamin B_6, 2.5 mg; vitamin B_{12}, 0.015 mg; pantothenic acid calcium, 12.5 mg; nicotinic acid, 32.5 mg; folic acid, 1.25 mg; biotin, 0.125 mg; choline, 700 mg; Zn ($ZnSO_4 \cdot 7H_2O$), 60 mg; Fe ($FeSO_4 \cdot 7H_2O$), 80 mg; Cu ($CuSO_4 \cdot 5H_2O$), 8 mg; Mn ($MnSO_4 \cdot H_2O$), 110 mg; I (KI), 0.35 mg; Se (Na_2SeO_3), 0.15 mg. Premix provided per kilogram of diet for 4 to 6 wk: vitamin A, 10,000 IU; vitamin D_3, 3,400 IU; vitamin E,16 IU; vitamin K_3, 2.0 mg; vitamin B_1, 2.0 mg; vitamin B_2, 6.4 mg; vitamin B_6, 2.0 mg; vitamin B_{12}, 0.012 mg; pantothenic acid calcium, 10 mg; nicotinic acid, 26 mg; folic acid, 1 mg; biotin, 0.1 mg; choline, 500 mg; Zn ($ZnSO_4 \cdot 7H_2O$), 40 mg; Fe ($FeSO_4 \cdot 7H_2O$), 80 mg; Cu ($CuSO_4 \cdot 5H_2O$), 8 mg; Mn ($MnSO_4 \cdot H_2O$), 80 mg; I (KI), 0.35 mg; Se (Na_2SeO_3), 0.15 mg.

[2]ME was calculated according to the data of Chinese Feed Database (2018), whereas the others were measured.

Metabolites Identification and Pathway Analysis

The Metlin database was used to identify potential specific biomarker candidates based on their MS signature and tandem mass spectrometry (MS/MS) spectra, as well as eventual contaminants. Identification of potential biomarkers was carried out by searching METLIN (http://metlin.scripps.edu/), HMDB (http://www.hmdb.ca/), KEGG (http://www.genome.jp/kegg/), MassBank (http://www.massbank.jp/), LIPIDMAPS (http://www.lipidmaps.org/), and Chemspider (http://www.chemspider.com) using the exact molecular weights or the MS/MS fragmentation pattern data, and a literature search was conducted to identify the affected metabolic pathways and to facilitate further biological interpretation. Mass accuracy tolerance within 25 ppm was used as the mass window for the database search. For confirmation of the metabolite identities using an authentic chemical standard, the MS/MS fragmentation pattern of the chemical standard was compared with that of the candidate metabolite under the same LC-MS conditions to reveal any matching. In the case of unknown metabolites, molecular formulae were generated using the Mass Profiler Professional (Agilent Technologies).

Statistical Analysis

Data on growth performance; respiratory rate; core body temperature; skin temperature of leg, flipper, earlobe, comb, and eyelids; blood glucose; muscle glycogen; liver glycogen, T_3, T_4, CORT, AKP, CK, HSP70, and av UCP mRNA were analyzed using the one-way anova procedure in SAS version 9.2 (SAS Institute Inc., Cary, NC). Differences among means were

tested using Duncan's multiple range test. Replicate cage served as the experimental unit, and $P < 0.05$ was considered to be statistically significant.

RESULTS

Growth Performance

RH stress reduced the growth performance in the experiment broilers (Figure 1). Eighty-five percent RH decreased ($P < 0.02$) the average daily feed intake, and both 35 and 85% RH decreased ($P < 0.01$) the ADG.

Glucose, Glycogen, Urea Levels

RH had effects ($P < 0.05$) on the blood glucose, muscle glycogen, and blood urea and had no effect ($P > 0.06$) on the hepatic glycogen (Figure 2). Eighty-five percent and 35% RH increased ($P < 0.0001$) the blood glucose, and the 85% RH further increased ($P < 0.05$) it compared with the 35% RH, and both decreased ($P < 0.05$) the muscle glycogen. Thirty-five percent RH increased ($P = 0.05$) the blood urea.

Serum Hormones and Hypothalamus HSP70 Concentrations

RH had effects ($P < 0.05$) on the T_3, T_4, CORT, AKP, and CK (Figure 3). Eighty-five percent RH increased ($P < 0.03$) the T_3 compared with the 35% RH. Eighty-five percent and 35% RH increased ($P < 0.03$) the T_4 in serum. Thirty-five percent RH decreased ($P < 0.0001$) the CORT in serum compared with the other groups. Eighty-five percent RH increased ($P = 0.0298$) the AKP in serum compared to the other groups. Eighty-five percent and 35% RH increased ($P < 0.02$) the CK in serum. Thirty-five percent RH decreased ($P = 0.0364$) the HSP70 in hypothalamus compared to the other groups.

Av UCP Expression, Respiratory Rate, Skin Temperature, and Core Body Temperature

RH had an effect ($P < 0.05$) on the av UCP expression (Figure 4A). Compared with the 60% RH, both 85 and 35% RH increased ($P < 0.05$) the av UCP expression. RH also had effects ($P < 0.01$) on the respiratory rate, skin temperature, and core body temperature (Figure 4B–H). Compared with the 60% RH, 85% RH increased ($P < 0.0001$) the respiratory rate, and 35% RH decreased ($P < 0.0001$) it; however, 85% RH decreased ($P < 0.01$) the skin temperature (leg, flipper, earlobe, comb, eyelid), and 35% RH increased ($P < 0.01$) it. Eighty-five percent RH increased ($P < 0.05$) the core body temperature.

Fecal Metabolic Profiling by UHPLC-Q-TOF/MS

The stability of the analytical method is crucial for obtaining valid metabolomics data. To validate the system's performance during sample analysis, a pooled QC sample was applied that was a representative "mean" sample including all analytes used during the analysis (Sangster et al., 2006). QC samples were handled as real samples and inserted every 5 samples into the ESI positive or negative analysis batch to monitor the stability of the instrument. The similarity of the QCs included the peak shape, separation degrees, retention times, and intensity distribution of the metabolites involved in the profiles. The results indicated that the method was robust with good repeatability and stability, rather than the product of artefacts arising from technical errors, and was suitable for the measurement of the samples in this study.

Using the XCMS software for peak detection, 10,113 peaks of positive ions and 10,685 negative ions in RPLC, 4,186 peaks of positive ions and 10,014 negative ions in HILIC were obtained. Although fewer peaks were extracted from the HILIC column, these peaks can also be used as a comprehensive fecal metabolomics profiling as well as RPLC. The variables were exported into MetaboAnalyst for multivariate data analysis to detect any inherent trend within the date. All fecal samples were divided into 3 groups: G1, 35% RH (hot-dry) group; G3, 60% RH (hot-mid) group; and G5, 85% RH (hot-humid) group. A PCA was carried out using these molecular features on all the sample groups from the study including conditioning runs and QC samples. The distribution of metabolic profiles for the QC samples in PCA can be seen in Figure 6. All the QC injections (Green) were clustered tightly in the PCA space. The consistency of the repeated QC injections and reliable data quality across all the samples demonstrated the suitability of the method for metabolic profiling studies during the experiment.

The separation conditions of fecal samples on both columns were optimized. Typical UHPLC-Q-TOF/MS total ion current chromatograms of fecal samples from the G1 group, G3 group, and G5 group in both positive- and negative-ion modes were shown in Figures 7, 8. Under experimental conditions, the total ion current shared considerable similarity, and the peak shape of each substance was good and the peaks well separated from each other, indicating that the chromatographic and MS conditions were suitable for the measurement of the samples in this study. RPLC has better retention for weakly polar component. In addition, HILIC allows varied selectivity and the better retention for polar analytes. The integrated utilization of 2 separation modes could enlarge metabolite identification.

Normalization and Multivariate Statistical Analysis

It is often necessary to normalize metabolomics data before starting any kind of statistical analysis. Normalization can reduce any systematic bias or technical variation, and metabolite concentrations usually span several orders of magnitude, which can lead to misidentification of significant changes. In our study, the "50% rule" was applied to remove the missing values, and the

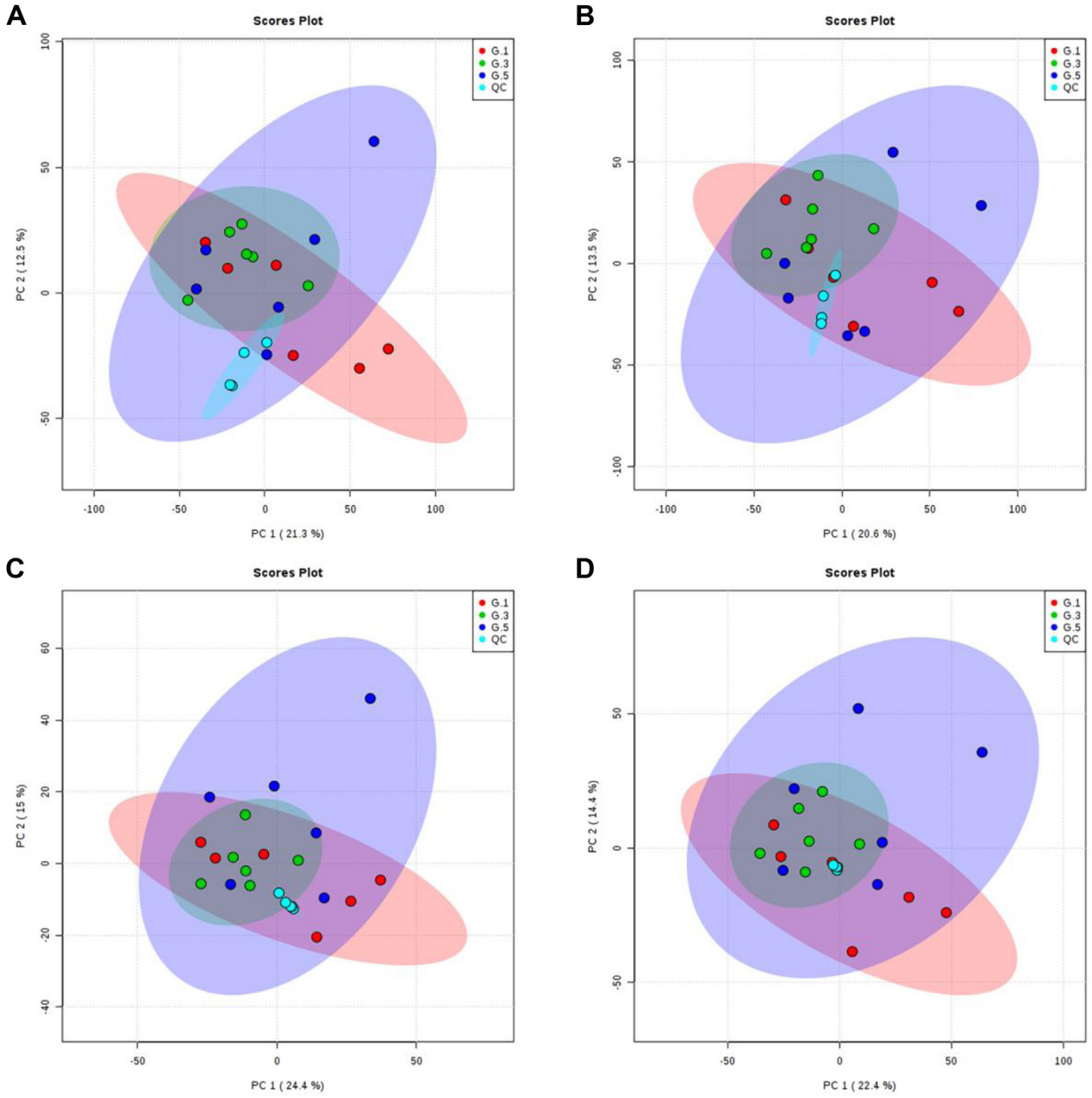

Figure 6. Principle component analysis (PCA) score plots in electrospray ionization (ESI)-positive mode of HSST3 (A), negative mode of HSST3 (B), positive mode of HILIC (C), and negative mode of HILIC (D) based on the ultra-high-performance liquid chromatography coupled with quadrupole time-of-flight mass spectrometry (UHPLC-Q-TOF/MS) data of the fecal samples.

results indicated that the metabolomics data presented a normal distribution after normalization processing (Figure 9).

Principal Component Analysis

To determine whether the global metabolite fingerprints in fecal differed among the hot humid (G5), mid (G3), or dry (G1) treatments, we evaluated the separation among the 3 treatments in both ion modes using unsupervised PCA. PCA is an unsupervised clustering or classification method. PCA showed that 42.4% of the total variance in the data was represented by the first 2 principal components in the positive mode in HILIC (Figure 10A). The total variance in the data represented by the first 2 principal components in the negative mode in HILIC was 39.6% (Figure 10B). However, the total variance in the data represented by the first 2 principal components in the positive and negative in RPLC were 35.9% and 36%, respectively (Figures 10C, 10D). In these plots, compared to the G1 and G3 groups, G5 group showed a slight but not significant separation trend in the 2D-PCA score plots. The plot revealed that the trend of G1 and G3 separation was not obvious in positive and negative ion mode data, but there was a significant trend in the G5 group, which indicated that G5 group had some changes in metabolic profile.

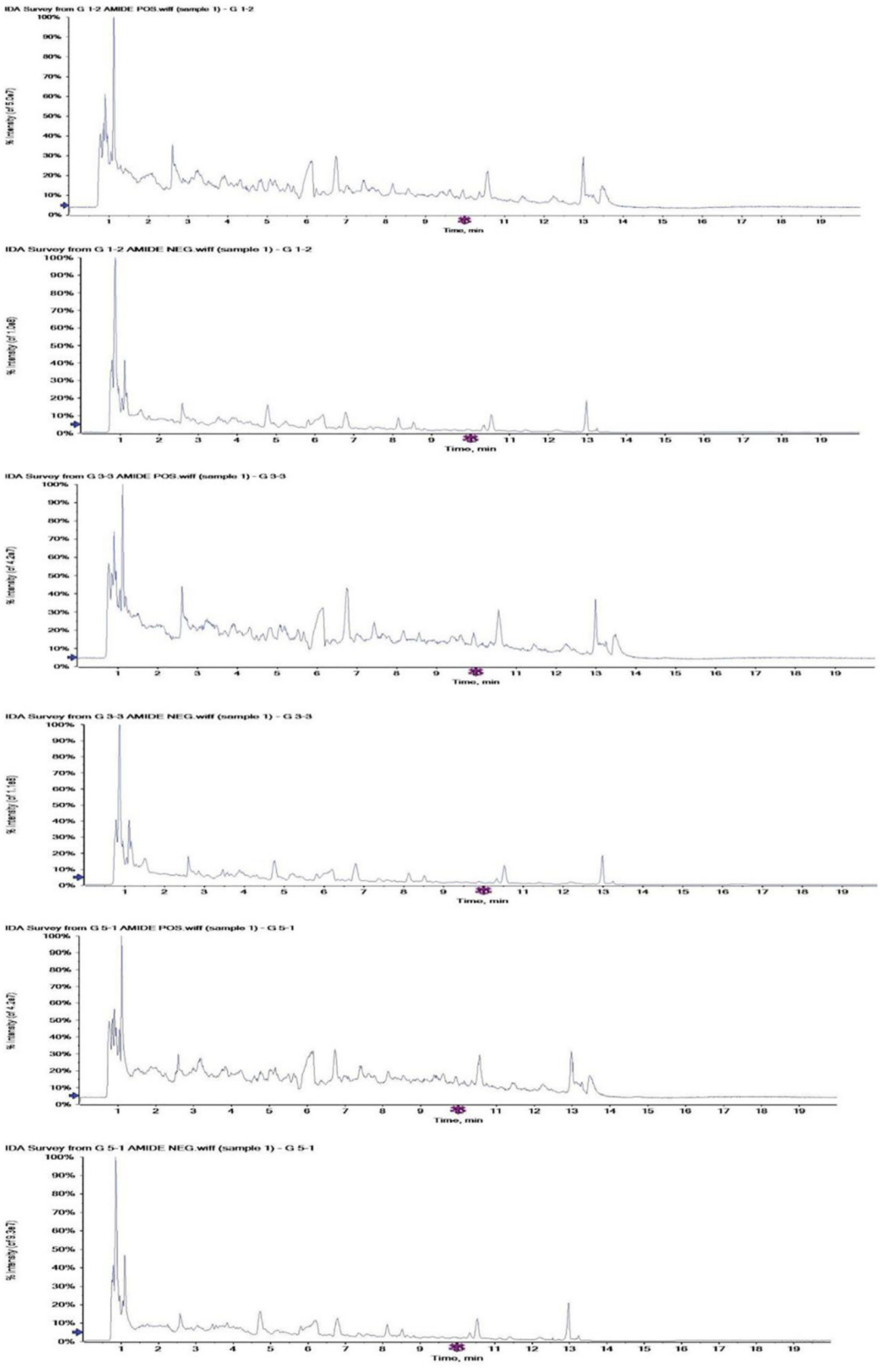

Figure 7. Representative total ion chromatograms (TICs) of fecal samples obtained by LC-MS analysis in the HILIC.

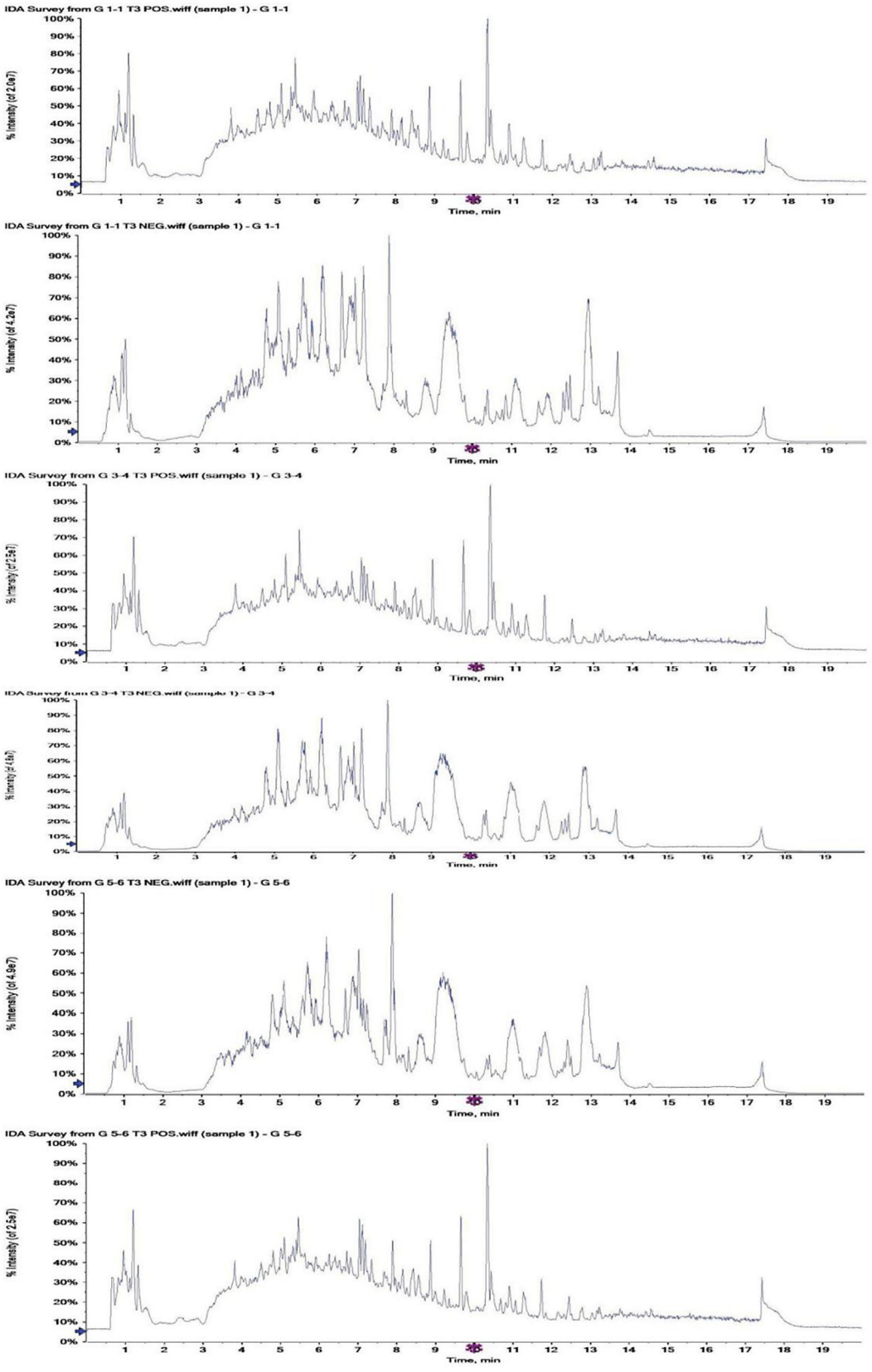

Figure 8. Representative total ion chromatograms (TICs) of fecal samples obtained by LC-MS analysis in the HSST3.

Partial Least Squares Discrimination Analysis

To further identify ion peaks that could be used to discriminate among the hot-humid (G5), mid (G3), or dry (G1) treatments, a supervised PLS-DA model was established that was more focused on the actual class discriminating variation than the unsupervised PCA model. PLS-DA is a supervised clustering or classification method. PLS-DA projects the data into a low-

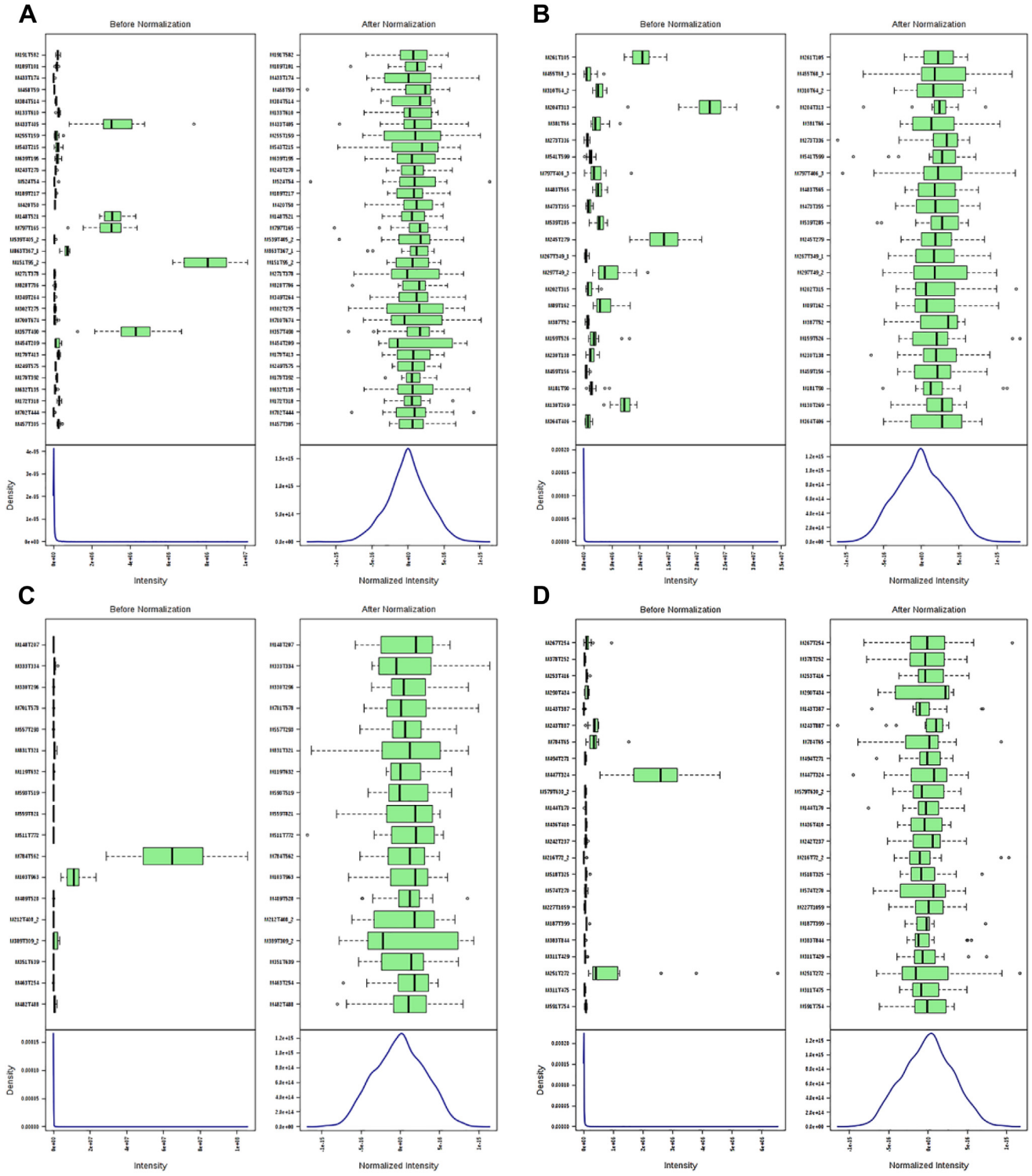

Figure 9. This graph summarizes the distribution of input data values before and after normalization: (A) positive mode of HILIC, (B) negative mode of HILIC, (C) negative mode of HSST3, (D) positive mode of HSST3.

dimensional space that maximizes the separation among different groups in the latent variables.

Supervised analysis, PLS-DA, was subsequently performed to maximize the separation and identify the metabolites. A clear separation among the G1, G3, and G5 groups was observed based on the PLS-DA score plot by the first 2 components in the positive ion mode (HILIC: R2 = 0.960, Q2 = 0.564; HSS T3: R2 = 0.886, Q2 = 0.163) (Figures 11A, 11C) and negative ion mode (HILIC: R2 = 0.935, Q2 = 0.455; HSS T3: R2 = 0.955, Q2 = 0.278) (Figures 11B, 11D) (indices representing the goodness of the fit [R2] and the prediction ability of the model [Q2]). The models allow for a satisfactory clustering trends among the G1, G3, and G5 groups, indicating the possibility of using fecal metabolomics for evaluating stress. From these score

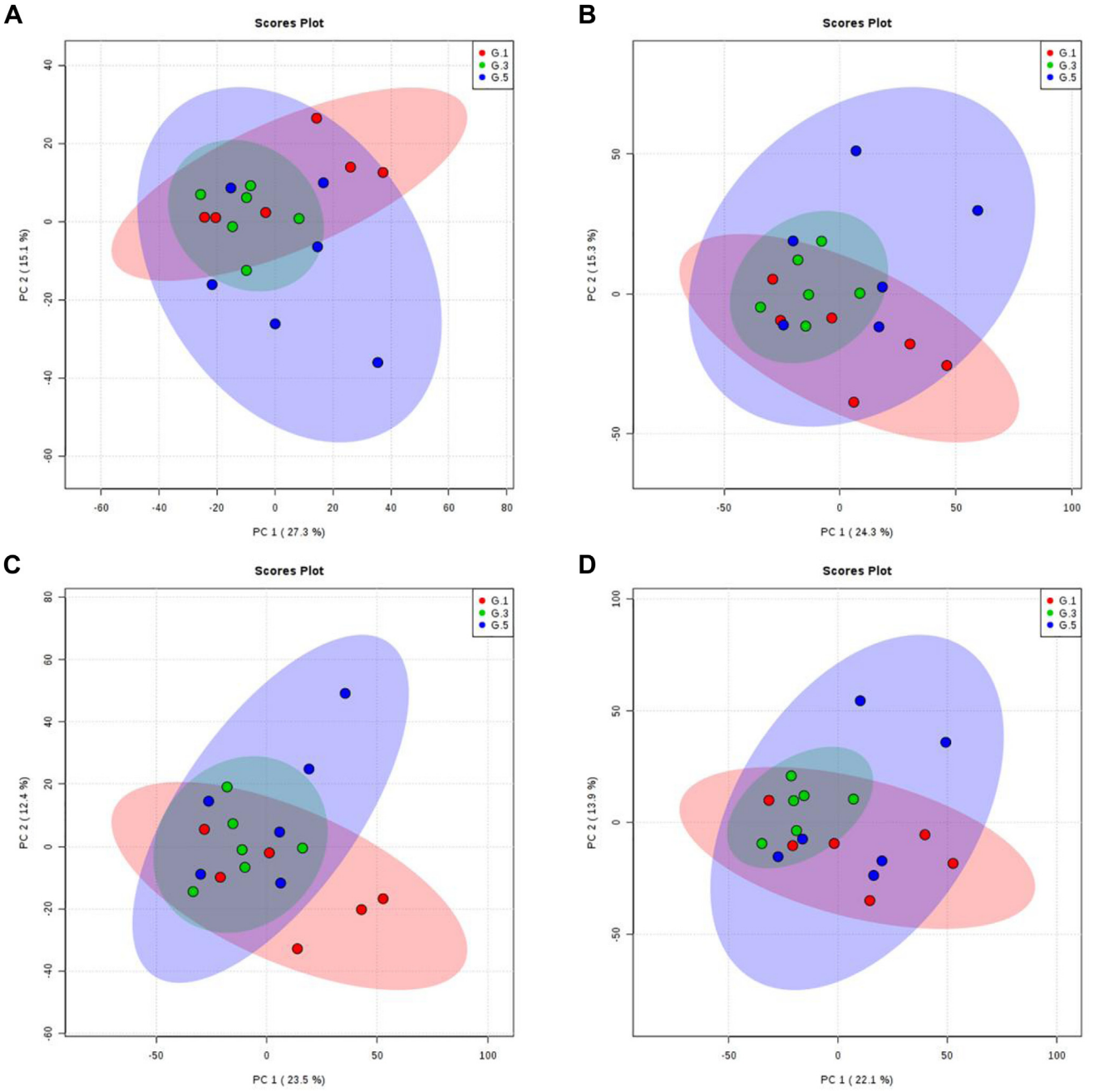

Figure 10. Principle component analysis (PCA) score map derived from ultra-high-performance liquid chromatography coupled with quadrupole time-of-flight mass spectrometry (UHPLC-Q-TOF/MS) spectra concerning G1 (red dot), G3 (green dot), G5 (blue dot) in the positive mode of HILIC (A), negative mode of HILIC (B), positive mode of HSS T3 (C), and negative mode of HSS T3 (D).

plots, we found that regardless of whether looking at either the PCA or PLS-DA score plots, the separation trend among the 3 groups was good in both positive and negative modes of HILIC and HSS T3, which indicates that different levels of RH at high-temperature Mn result in some changes in the levels of a few metabolites.

Detection and Identification of Differential Metabolites

To identify which variables were responsible for this separation, a study on the variable influence on the projection parameter was conducted. VIP values calculated using the PLS-DA model revealed which variables (metabolites) had the greatest influence on the discrimination between the fecal metabolic samples. Potential metabolites were selected based on the VIP score (>1). For the univariate analysis, candidate-specific biomarkers were determined using single-dimensional statistical one-way ANOVA analysis. The critical P value was set to 0.05 for the significantly differential variables in this study. We searched for candidates from the freely accessible databases of HMDB (http://www.hmdb.ca), METLIN (http://metlin.scripps.edu), and KEGG (http://www.kegg.jp) by their masses, then, MS/MS analyses were performed, and owing to the possible fragment mechanisms,

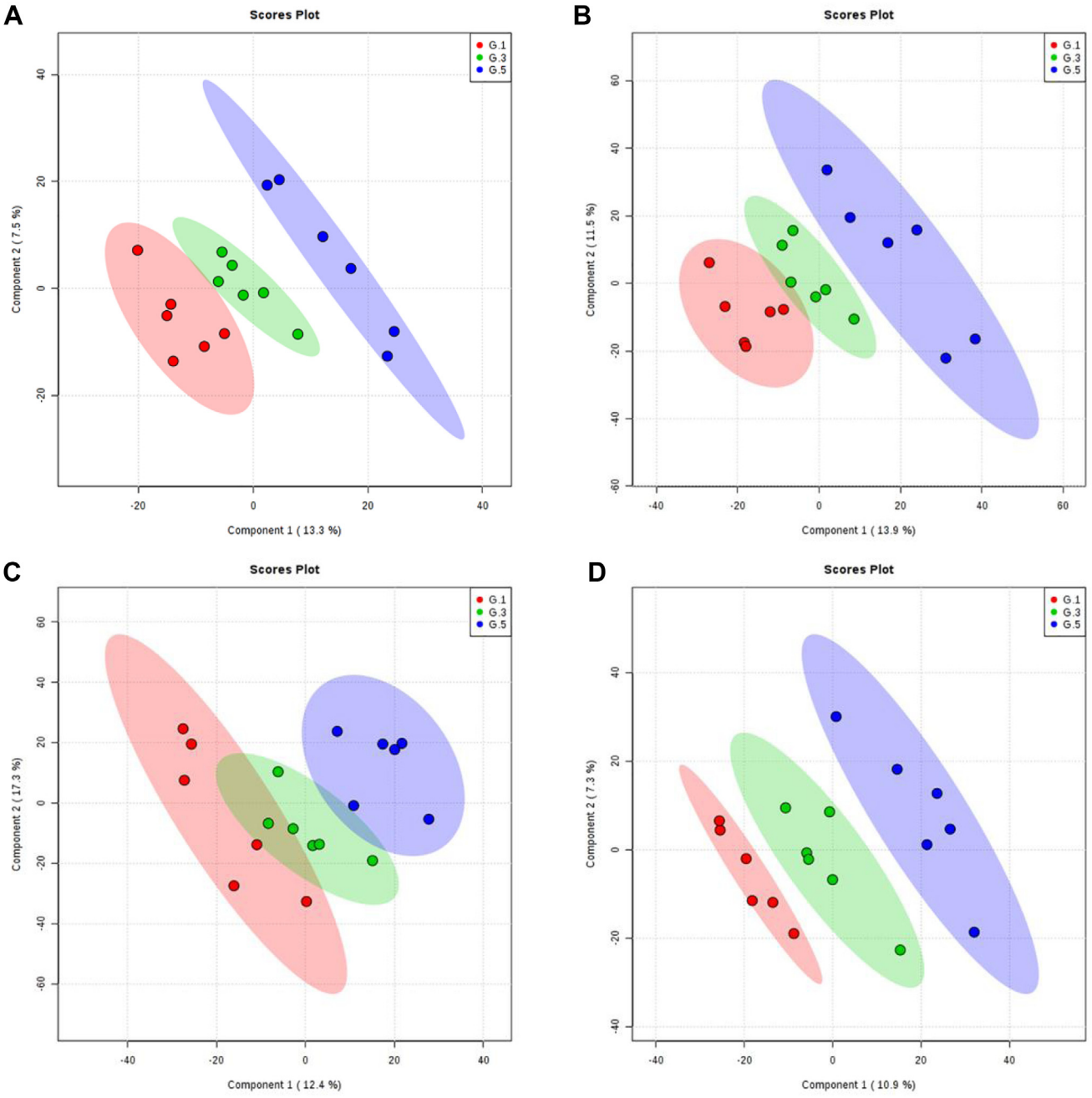

Figure 11. Partial-least squares discrimination analysis (PLS-DA) score map derived from ultra-high-performance liquid chromatography coupled with quadrupole time-of-flight mass spectrometry (UHPLC-Q-TOF/MS) spectra concerning concerning G1 (red dot), G3 (green dot), G5 (blue dot) in the positive mode of HILIC (A), negative mode of HILIC (B), positive mode of HSS T3 (C), and negative mode of HSS T3 (D).

items without given mass fragment information were removed from the candidate list and only the most probable items were left. By comparing the retention times and mass spectra of the authentic chemicals as well as the standard MS/MS spectra from the aforementioned databases, 36 significantly differential fecal metabolites were selected as potential biomarkers related to hot-humid, mid, or dry stress (Tables 2 and 3). Tables 2 and 3 also shows the tentative identification of these metabolites (compound name, molecular formula, adduct). The metabolites of uracil, hydroxyproline, 2-isopropylmalic acid, xanthine, benzoic acid, 1,4-dihydroxybenzene, DL-methionine sulfoxide, thymine, adenine, taurocholate, and so on may be potential biomarkers for hot-humid, mid, or dry stress based on their VIP scores. The greater the VIP score of the metabolite, the greater the contribution to the separation of sample classification; therefore, the metabolite may be a potential biomarker (Ma et al., 2014; Wang et al., 2017).

In general, when the screening of the metabolites was reasonable and accurate, the samples from one group appeared in one cluster. Metabolites gathered in the same cluster had similar patterns of expression, which may indicate that they were involved in adjacent or close steps in the overall process of metabolism. The tree structure on the left side of Figure 12 represented the

Table 2. Samples of HILIC cation and anion G1-G3-G5 group of chicken manure to identify differences in metabolites.

Ionization mode (HILIC)	Adduct	VIP	*P* value	m/z	Retention time (s)	Formula	Metabolite
ESI(+)	(M + NH4)+	1.6567	0.024099	533.3251	107.138	$C_{26}H_{45}NO_7S$	Taurocholate
ESI(+)	(M + CH3COO+2H)+	1.1165	0.025783	251.1387	158.951	$C_6H_{14}N_4O_3$	N-(omega)-hydroxyarginine
ESI(+)	(M + H)+	1.8343	0.011604	130.0496	448.408	$C_5H_7NO_3$	L-Pyroglutamic acid
ESI(+)	(M + H)+	2.8862	0.016132	132.0663	385.740	$C_5H_9NO_3$	Hydroxyproline
ESI(+)	(M + H)+	1.0334	0.016313	112.0869	107.218	$C_5H_9N_3$	Histamine
ESI(+)	(M + H)+	2.0389	0.003919	147.076	448.394	$C_5H_{10}N_2O_3$	L-Glutamine
ESI(+)	(M + H)+	2.137	0.027125	201.9836	302.696	$C_3H_7NO_5S_2$	Cysteine-S-sulfate
ESI(+)	(M + H-H2O)+	1.8167	0.014495	241.0927	90.538		Acadesine (drug)
ESI(+)	(M + H)+	2.0528	0.008267	146.0928	410.597	$C_5H_{11}N_3O_2$	4-Guanidinobutyric acid
ESI(+)	(M + H)+	1.0994	0.002954	126.1025	383.346		l-Methylhistamine
ESI(-)	(M-H)-	3.0329	0.001232	111.0203	88.403	$C_4H_4N_2O_2$	Uracil
ESI(-)	(M-H)-	1.6072	0.011230	514.2802	103.059	$C_{26}H_{45}NO_7S$	Taurocholate
ESI(-)	(M-H)-	2.1443	0.040660	117.0204	505.952	$C_4H_6O_4$	Succinate
ESI(-)	(M + CH3COO)-	1.8129	0.003737	725.2303	746.889	$C_{24}H_{42}O_{21}$	Stachyose
ESI(-)	(M-H)-	1.1399	0.031148	115.0034	160.740	$C_4H_4O_4$	Maleic acid
ESI(-)	(M-H)-	2.3313	0.002030	128.0351	386.61	$C_5H_7NO_3$	L-Pyroglutamic acid
ESI(-)	(M-H)-	2.4013	0.045091	181.0500	161.396	$C_9H_{10}O_4$	Hydroxyphenyllactic acid
ESI(-)	(M-H)-	2.2755	0.033835	193.0355	497.042	$C_6H_{10}O_7$	D-galacturonic acid
ESI(-)	(M-H)-	2.0934	0.025000	199.9690	300.059	$C_3H_7NO_5S_2$	Cysteine-S-sulfate
ESI(-)	(M-H)-	1.0862	0.030828	145.0503	489.616	$C_6H_{10}O_4$	Adipic acid
ESI(-)	(M-H)-	1.9144	0.046224	163.0400	107.911	$C_9H_8O_3$	4-Hydroxycinnamic acid
ESI(-)	(M-H)-	3.1972	0.01728	175.0610	394.802	$C_7H_{12}O_5$	2-Isopropylmalic acid

Abbreviation: VIP, variable importance in projection.

clustering relationships of each metabolite, and the tree structure at the top represents the clustering relationships of each sample. Hierarchical clustering results also showed that significantly different metabolites existed among the 3 groups, although some metabolites also showed similarities.

Potential Metabolic Pathways Related to the Hot-Humid, Mid, or Dry Stress

Pathway analysis has been proven to be an invaluable tool for understanding complex relationships among genes and proteins (Goffard et al., 2009; Hu et al., 2009). Therefore, to identify possible pathways relevant to the hot-humid, mid, or dry stress, all the attributed metabolites were subjected to Metaboanalyst 3.0, a free online tool based on the high-quality KEGG metabolic pathways database (www.metaboanalyst.ca). The influenced metabolic pathway was set as $P < 0.05$. Hence, 13 metabolic pathways were detected as potential metabolic pathways for the hot-humid, mid, or dry stress (Figure 13). With the power of this metabolomics analysis, the versatile effects of hot-humid, mid, or dry stress on the different metabolic pathways in fecal samples could be observed in an untargeted manner. The results showed that the potential biomarkers were responsible for primary bile acid biosynthesis, taurine and hypotaurine metabolism, phenylalanine metabolism, histidine metabolism, tyrosine metabolism, pyruvate metabolism, beta-alanine metabolism, and so on (Table 4). The different metabolic pathways were likely due to the dynamic process of hot-humid, mid, or dry stress and might be closely associated with RH stress.

DISCUSSION

To the best of our knowledge, this is the first study to identify metabolic pathways associated with the hot-humid or dry climate in broilers. In our study, we analyzed the main pathways affected by hot-humid, mid, or dry stress. Such analysis enabled us to explain the route of how hot-humid or dry climate decreased

Table 3. Samples of HSST3 cation and anion G1-G3-G5 group of chicken manure to identify differences in metabolites.

Ionization mode (HSST3)	Adduct	VIP	*P* value	m/z	Retention time (s)	Formula	Metabolite
ESI(+)	(M + H)+	2.885	0.0459731	153.0407	140.121	$C_5H_4N_4O_2$	Xanthine
ESI(+)	(M + H)+	1.159	0.0348263	516.3009	451.884	$C_{26}H_{45}NO_7S$	Taurocholate
ESI(+)	(M + H)+	2.303	0.00147405	281.1152	276.2585	$C_{13}H_{16}N_2O_5$	L-Aspartyl-L-phenylalanine
ESI(+)	(M + H)+	2.722	0.00231868	166.0538	52.196	$C_5H_{11}NO_3S$	DL-Methionine sulfoxide
ESI(+)	(M + H-H2O)+	2.165	0.0375587	241.0942	224.479		Acadesine (drug)
ESI(-)	(M-H)-	3.1789	0.004477	111.0188	71.9575	$C_4H_4N_2O_2$	Uracil
ESI(-)	(M-H)-	2.6688	0.001702	125.0343	202.795	$C_5H_6N_2O_2$	Thymine
ESI(-)	(M-H)-	2.4173	0.006158	514.2805	359.21	$C_{26}H_{45}NO_7S$	Taurocholate
ESI(-)	(M-H)-	1.821	0.048278	212.0004	243.728	$C_{14}H_{17}NO_6$	Indoxylsulfate
ESI(-)	(M-H)-	1.6296	0.041899	179.0334	204.091	$C_9H_8O_4$	Caffeic acid
ESI(-)	(M-H)-	3.1267	0.001074	121.0283	216.653	$C_7H_6O_2$	Benzoic acid
ESI(-)	(M-H2O-H)-	1.3353	0.028934	241.011	45.323	$C_6H_{13}O_9P$	alpha-D-Glucose 1-phosphate
ESI(-)	(M-H)-	2.6852	0.007368	134.0457	233.806	$C_5H_5N_5$	Adenine
ESI(-)	(M-H)-	3.5747	0.003354	109.0283	306.3185	$C_6H_6O_2$	1,4-Dihydroxybenzene

Abbreviation: VIP, variable importance in projection.

growth and supressed heat dissipation in broilers at the metabolic levels.

High RH or low RH at high temperatures increased gluconeogenesis and caused heat dissipation disorder and decreased broiler growth. We found significant reduction of ADG, increase of glucose and urea in blood (low RH), decrease of respiratory and increase of skin temperature (low RH), increase of respiratory rate and decrease of skin temperature (high RH), increase the expression of av UCP in muscle and body temperature in the low- and high-RH groups, as presented in Figure 1, Figure 2, Figure 4, respectively. However, the mechanism of their metabolic changes caused by RH was obscure. Therefore, in the subsequent step, the metabolic pathway affected by RH was investigated. As shown in Figure 13, metabolic pathways were detected, which were related to the decreased growth and supressed heat dissipation. We found that pyruvate metabolism, galactose metabolism and ABC transporter, aminoacyl-tRNA biosynthesis, primary bile acid biosynthesis and taurine and hypotaurine metabolism, arginine and proline metabolism, and histidine metabolism were affected by RH. All these pathways were associated with growth decline and heat dissipation.

Pyruvate, an intermediate metabolite of the gluconeogenesis pathway, plays an important role in energy metabolism (Chen et al., 2011) and is the end product of glycolysis and the starting substrate for the tricarboxylic acid cycle (Chang et al., 2018). Previous studies showed that creatine pyruvate improved the energy status, increased the gene expression of glucose transporter proteins, and facilitated glycolysis in breast muscle (Zhao et al., 2018). In the present study, succinic acid, pyruvic aldehyde, and 2-isopropylmalic acid were involved in the pyruvate metabolic pathway. Succinic acid is an important product in the process of the tricarboxylic acid cycle. Pyruvic aldehyde is a metabolite in the glycolysis process. These substances were important metabolites in the process of glucose metabolism, which indicated that RH stress can cause changes in the glucose metabolism of broilers, and combined with our biochemical indicators, hepatic glycogen, muscle glycogen, blood glucose, and urea of broilers have also changed, further indicating that RH caused the increased gluconeogenesis. In addition, the pathway involved in glucose metabolism is galactose metabolism. Its metabolism was mainly through galactose kinase, galactose-1-phosphate uridine transferase, and urine. The glycoside diphosphate galactose-4-differase and its catalyzed enzymatic reaction were converted to glucose and used. In this study, it was found that α-D-glucose 1-phosphate, stachyose, and d-(+)-meliose in the metabolites were involved in the galactose metabolism pathway. At the same time, it was found that the RH stress caused a change in the metabolism of the adenosine triphosphate–binding cassette transporter (ABC transporter). The ABC transporter was named for its binding cassette containing ATP. ABC transporter is a membrane integrin that uses the energy of hydrolyzing ATP to facilitate transmembrane transport of various biomolecules in solute. The substrates for transport include sugars, amino acids, metal ions, peptides, proteins, cellular metabolites, and drugs. In this study, L-glutamine, hydroxyproline, D-(+)-melose, D-galacturonic acid, and L-phenylalanine were found to be involved in the ABC transporter metabolic pathway. Alanine is a precursor of synthetic carnosine, which acts as an ionic buffer and improves glucose metabolism (Yu et al., 2014). In this study, uracil and L-carnosine were found to be involved in the β-alanine metabolic pathway. The aforementioned results indicated that RH caused increased gluconeogenesis in broilers.

In the process of biotransformation, each tRNA molecule needs to bind to the corresponding amino acid and then transport these amino acids to the ribosome for protein synthesis. The bond formed between the amino acid and the tRNA is a high-energy bond, called an aminoacyl-tRNA bond, which plays an important role in transport. If the aminoacyl-tRNA synthesis is impaired, the synthesis of the protein will inevitably be affected, which will further affect the hormones secretion, enzyme synthesis, protein synthesis, cell proliferation, and so on. In the present study, 3 metabolites of L-methionine, L-glutamine, and L-phenylalanine were involved in the aminoacyl-tRNA anabolic pathway, which indicated that the protein translation process is involved in the RH stress and the various hormones that cause secretion are hampered, and at the same time, we measured the amount of some serum enzymes and found that the contents of AKP, CK, T_3, T_4, CORT, and HSP70 changed. The aforementioned results indicated that RH caused protein synthesis and hormone secretion disorders.

Taurine, 2-aminoethanesulfonic acid, is an abundant β-amino sulfonic acid in many excitable tissues. It presents as a free form, accounting for approximately 0.1% of the total body mass (De Luca et al., 2015; Lambert et al., 2015; Schaffer and Kim, 2018). Previous studies indicate that taurine exerts important physiological functions in modulation of intracellular calcium concentration, ion channel function, glucose and lipid homeostasis, cellular redox homeostasis, and antiantioxidant and anti-inflammatory responses (Li et al., 2017; Ribeiro et al., 2018; Seidel et al., 2018). In this study, significant changes were observed in the metabolic pathway of taurine and hypotaurine, and taurocholate was involved in this pathway. In addition, it has also been found that the biosynthetic metabolic pathway of primary bile acids has also changed significantly. There were 9 (taurine deoxycholate, tauro-goose (deoxy) cholate, taurocholate, cholic acid, and so on) metabolites enriched in this pathway, it can be inferred that RH stress can cause changes in the metabolism of bile acids in the liver, affecting the absorption of lipids and fat-soluble vitamins, which in turn influences the synthesis of fat, thus reducing the growth of broilers.

Tyrosine is a synthetic precursor of the neurotransmitters norepinephrine, dopamine, and adrenergic receptors. These neurotransmitters play important neurotransmitters in the sympathetic nervous system. Once damaged, the overall signal transmission is affected

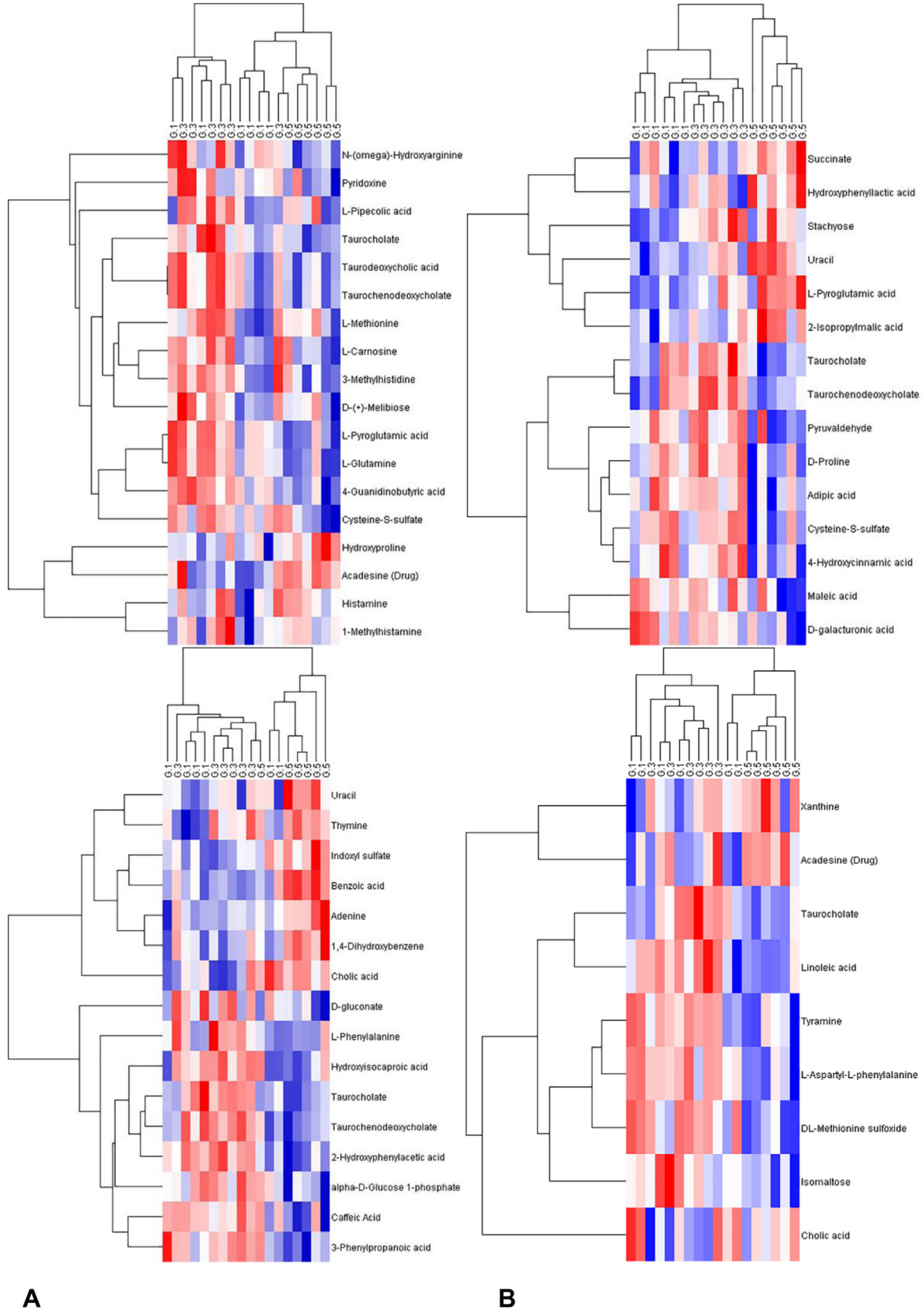

Figure 12. Hierarchically clustered heat map showing relative increase/decrease of metabolite contents and their similarities between individual samples. Columns correspond to different groups, and rows correspond to the altered metabolites. The heatmaps were constructed based on the metabolites of importance. Color key indicates metabolite expression value; blue: lowest, red: highest. (A) Positive mode of HILIC. (B) Negative mode of HILIC. (C) Negative mode of HSST3. (D) Positive mode of HSST3.

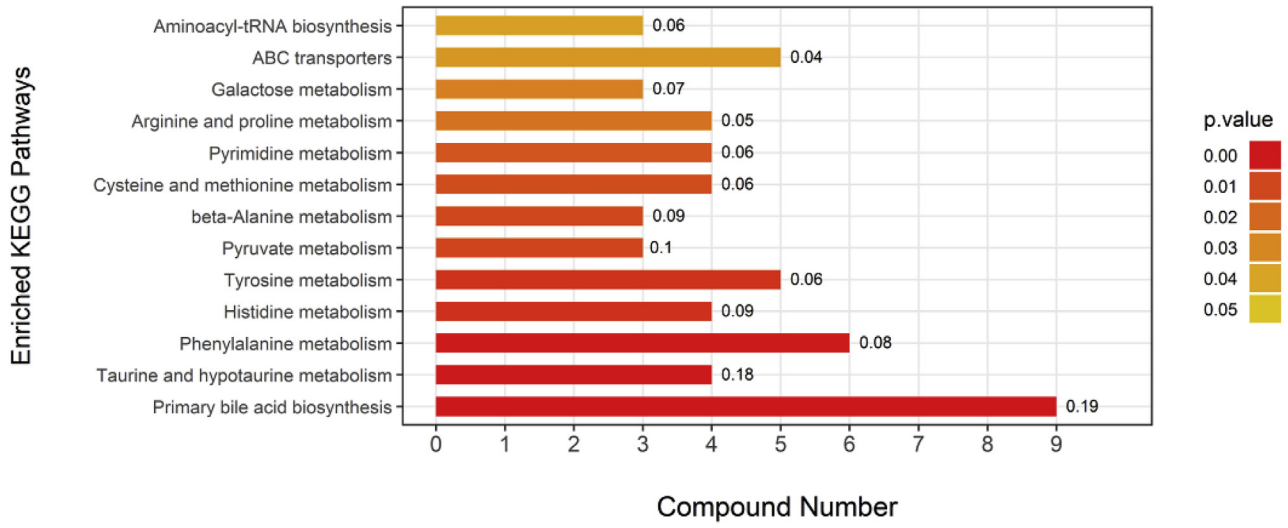

Figure 13. Enriched KEGG pathways. The x-axis represents the compound number of differential metabolites contained in each KEGG pathway, and y axis represents the pathway enrichment. The label above the bar graph shows the rich factor (rich factor ≤ 1). Larger sizes and darker colors represent higher pathway impact values and higher pathway enrichment.

(Rasmussen et al., 1983; Deijen and Orlebeke, 1994). In addition, tyrosine is a synthetic precursor of hormones, thyroids, and colorants (melanin) (Clark, 2015). It can also be converted into dopamine or catecholamine for signal transduction, or it can form a protein-activating enzyme with a phosphate group, regulate the activity of the enzyme, and provide energy (Held, 2006; Felger et al., 2013; Ramos et al., 2013). The catabolism of tyrosine involves the enzymatic, energy metabolism of the Krebs cycle. In this study, succinic acid, maleic acid, 4-hydroxycinnamic acid, tyramine, and 1,4-dihydroxybenzene were found to be involved in the tyrosine metabolic pathway. In addition, phenylalanine is an essential aromatic amino acid. Under normal circumstances, it is mainly metabolized in the liver and other tissues to produce tyrosine and then in the nervous system. The adrenal medulla synthesizes certain hormones, neurotransmitters such as dopamine, norepinephrine, epinephrine, and melanin in the skin. Therefore, the growth and development of the body and the maintenance of normal physiological functions require a stable state of phenylalanine metabolism. Insulin promotes uptake and utilization of branched-chain amino acids in muscle tissue and lowers blood glucose levels. Studies have found that (van Loon et al., 2000) phenylalanine can promote insulin secretion, which is believed to be

Table 4. Affected metabolic pathways including more than ≥3 metabolites (KEGG database matched results).

ID	Metabolic pathway name	Compound
map00120	Primary bile acid biosynthesis (9)	Taurodeoxycholic acid, taurochenodeoxycholate, taurocholate, taurochenodeoxycholate, taurocholate, cholic acid, taurocholate, taurochenodeoxycholate, cholic acid
map00430	Taurine and hypotaurine metabolism (4)	Taurocholate, taurocholate, taurocholate, taurocholate,
map00360	Phenylalanine metabolism (6)	Succinate, 4-hydroxycinnamic acid, L-phenylalanine, benzoic acid, 3-phenylpropanoic acid, 2-hydroxyphenylacetic acid
map00340	Histidine metabolism (4)	L-carnosine, histamine, 3-methylhistidine, 1-methylhistamine
map00350	Tyrosine metabolism (5)	Succinate, maleic acid, 4-hydroxycinnamic acid, tyramine, 1,4-dihydroxybenzene
map00620	Pyruvate metabolism (3)	Succinate, pyruvaldehyde, 2-isopropylmalic acid
map00410	beta-Alanine metabolism (3)	Uracil, L-carnosine, uracil
map00270	Cysteine and methionine metabolism (4)	L-Methionine, cysteine-S-sulfate, cysteine-S-sulfate, DL-methionine sulfoxide
map00240	Pyrimidine metabolism (4)	L-Glutamine, uracil, thymine
map00330	Arginine and proline metabolism (4)	N-(omega)-Hydroxyarginine, hydroxyproline, 4-guanidinobutyric acid, D-proline
map00052	Galactose metabolism (3)	D-(+)-Melibiose, stachyose, alpha-D-glucose 1-phosphate
map02010	ABC transporters (5)	L-Glutamine, hydroxyproline, D-(+)-melibiose, D-galacturonic acid, L-phenylalanine
map00970	Aminoacyl-tRNA biosynthesis (3)	L-Methionine, L-glutamine, L-phenylalanine

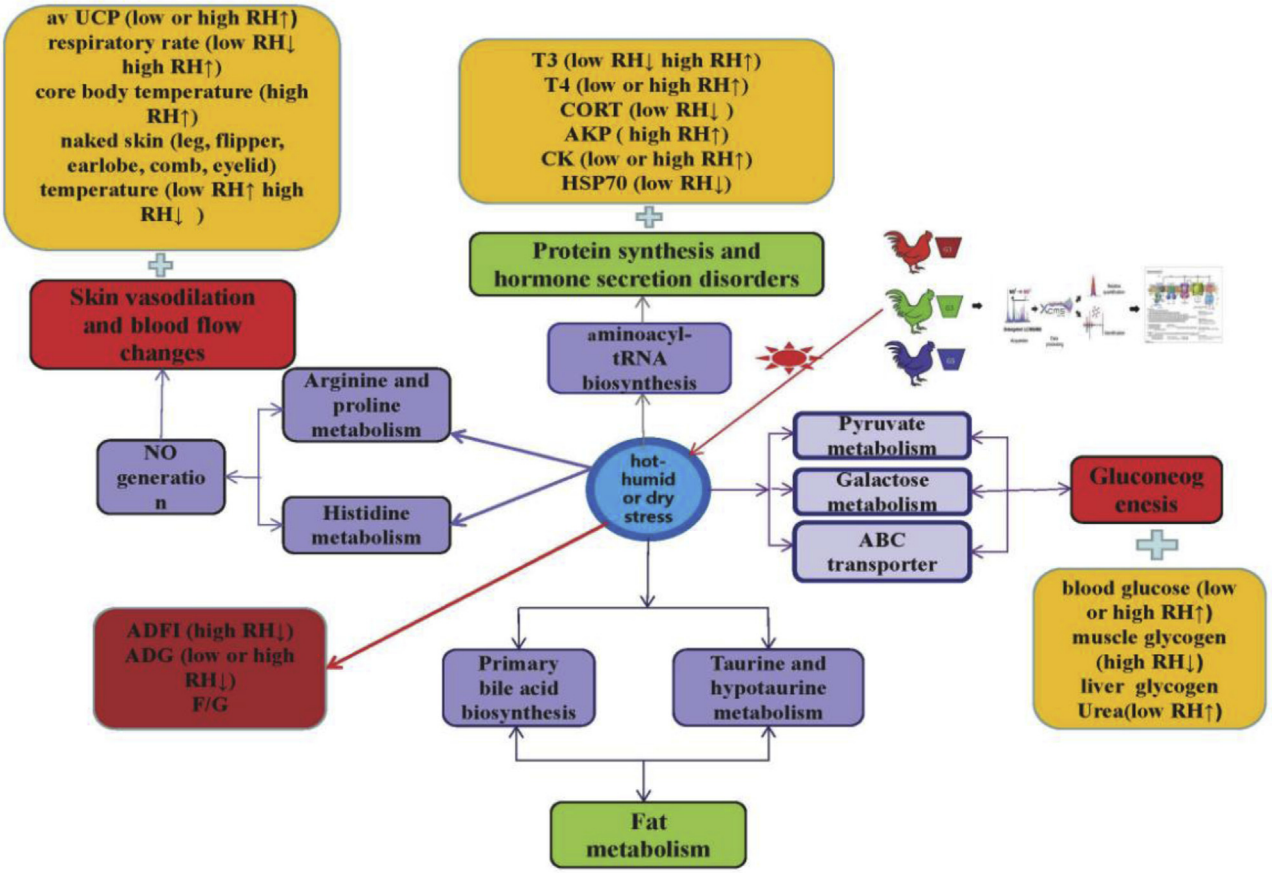

Figure 14. The metabolic network profile.

related to the increase in insulin levels as a nutrient supply to phenylalanine. In this study, it was found that succinic acid, 4-hydroxycinnamic acid, L-phenylalanine, benzoic acid, 3-phenylpropionic acid, and 2-hydroxyphenylacetic acid participate in the phenylalanine metabolic pathway. This also showed that RH stress can cause changes in hormones and glucose metabolism.

The maintenance of normal body temperature depends on the dynamic balance of the body's heat production and heat dissipation. The body continuously generates heat during metabolism to maintain body temperature. At the same time, the heat in the body is brought to the body surface by circulating blood, and the heat is dissipated by evaporation. Evaporative cooling depends on the temperature difference between the skin and the ambient temperature, which in turn is controlled by the blood flow of the skin. Therefore, the body can adjust the amount of body heat loss by changing the functional state of the skin blood vessels. Arginine is a precursor for the synthesis of many biomolecules, including ornithine, polyamines (putrescine, spermine, and spermidine), proline, glutamine, creatine, agmatine, NO, and proteins. Among them, NO is an endothelium relaxing factor released by vascular endothelial cells, which determines the blood flow of the skin. In this study, hydroxyproline, 4-mercaptobutyric acid, D-valine, and N-ω-hydroxyarginine were found to be involved in the arginine and proline metabolic pathways. In addition, histamine is one of autologous active substances and is abundant in the skin, bronchial mucosa, intestinal mucosa, and nervous system. The receptor that binds histamine to vascular smooth muscle (H1R) causes vasodilation and local edema. Histamine causes contraction of the tracheal smooth muscle of the lungs to cause airway stenosis and difficulty in breathing, and intestinal smooth muscle contraction lowers blood pressure and increases many physiological responses such as tachycardia. In this study, L-carnosine, histamine, 3-methylhistidine, and 1-methylhistamine were found to be involved in the histidine metabolism pathway. It can be seen that the RH stress would cause the blood flow of the skin to change, thereby changing the amount of heat dissipation and causing changes in body temperature. At the same time, we determined that the respiratory rate, body temperature, and skin temperature of broiler had changed (Figure 4). In addition, av UCP is a potential indicator of the energy inefficiency of ATP synthesis and energy metabolism (Masaki et al., 2000). Both high and low RH increased the expression of av UCP, which meant that the more the heat production to maintain body temperature, the less the energy used for growth.

In conclusion, this study investigated the metabolic signatures of the hot-humid, mid, or dry stress in broilers using an untargeted metabolomics platform combined with the serum metabolic changes or heat dissipation. Results from this global metabolic profiling study revealed the metabolic profile (Figure 14) in hot-humid or dry stress

broilers that might account for the pathway of pyruvate metabolism, galactose metabolism and ABC transporter, aminoacyl-tRNA biosynthesis, primary bile acid biosynthesis, and taurine and hypotaurine metabolism and also revealed the heat dissipation disorder that might be due to arginine and proline metabolism and histidine metabolism. Understanding the targets of these metabolites and metabolic pathway may improve our understanding of the adverse effects of hot-humid or dry climate on growing fast commercial broilers in the metabolic level and also the regulation of RH in poultry.

ACKNOWLEDGMENTS

This study was supported by the National Key Research and Development Program of China (2016YF D0500509).

Conflict of Interest Statement: The authors did not provide a conflict of interest statement.

REFERENCES

Adams, R. L., and J. C. Rogler. 1968. The effects of dietary aspirin and humidity on the performance of light and heavy breed chicks. Poult. Sci. 47:1344–1348.

Ayo, J. O., J. A. Obidi, and P. I. Rekwot. 2011. Effects of heat stress on the well-being, fertility and hatchability of chickens in the Northern Guinea Savannah zone of Nigeria: a review. ISRN Vet. Sci. 2011:1–10.

Benton, H. P., J. Ivanisevic, N. G. Mahieu, M. E. Kurczy, C. H. Johnson, L. Franco, D. Rinehart, E. Valentine, H. Gowda, B. K. Ubhi, R. Tautenhahn, A. Gieschen, M. W. Fields, G. J. Patti, and G. Siuzdak. 2015. Autonomous metabolomics for rapid metabolite identification in global profiling. Anal. Chem. 87:884–891.

Booth, S. C., M. L. Workentine, A. M. Weljie, and R. J. Turner. 2011. Metabolomics and its application to studying metal toxicity. Metallomics 3:1142–1152.

Chang, S. C., I. Lee, H. Ting, Y. J. Chang, and N. C. Yang. 2018. Parapyruvate, an impurity in pyruvate supplements, induces senescence in human fibroblastic Hs68 cells via inhibition of the α-Ketoglutarate dehydrogenase complex. J. Agric. Food Chem. 66:7504–7513.

Chen, J., M. Wang, Y. Kong, H. Ma, and S. Zou. 2011. Comparison of the novel compounds creatine and pyruvate on lipid and protein metabolism in broiler chickens. Animal 5:1082–1089.

Chinese Feed Database. 2018. Tables of feed composition and nutritive values in China. 29th ed. Chin. Feed.

Chwalibog, A., and B. O. Eggum. 1989. Effect of temperature on performance, heat production, evaporative heat loss and body composition in chickens. Arch. Geflugelkd. 53:179–184.

Clark, K. D. 2015. Altered tyrosine metabolism and melanization complex formation underlie the developmental regulation of melanization in manduca sexta. Insect Biochem. Mol. Biol. 58:66–75.

Dawkins, M. S., C. A. Donnelly, and T. A. Jones. 2004. Chicken welfare is influenced more by housing conditions than by stocking density. Nature 427:342–344.

De Luca, A., S. Pierno, and D. C. Camerino. 2015. Taurine: the appeal of a safe amino acid for skeletal muscle disorders. J. Transl. Med. 13:243.

Deijen, J. B., and J. F. Orlebeke. 1994. Effect of tyrosine on cognitive function and blood pressure under stress. Brain Res. Bull. 33:319–323.

FAO. 2010. Production: Livestock primary. Food and Agriculture Organization of the United Nations. Accessed Dec. 2010. http://faostat.fao.org/

Felger, J. C., L. Li, P. J. Marvar, B. J. Woolwine, D. G. Harrison, C. L. Raison, and A. H. Miller. 2013. Tyrosine metabolism during interferon-alpha administration: association with fatigue and CSF dopamine concentrations. Brain Behav. Immun. 31:153–160.

Gika, H. G., G. A. Theodoridis, J. E. Wingate, and I. D. Wilson. 2007. Within-day reproducibility of an HPLC−MS-based method for metabonomic analysis: application to human urine. J. Proteome Res. 6:3291–3303.

Goffard, N., T. Frickey, and G. Weiller. 2009. Path express update: the enzyme neighbourhood method of associating gene expression data with metabolic pathways. Nucleic Acids Res. 37:335–339.

Held, P. K. 2006. Disorders of tyrosine catabolism. Mol. Genet. Metab. 88:103–106.

Hu, Z., J. H. Hung, Y. Wang, Y. C. Chang, C. L. Huang, M. Huyck, and C. DeLisi. 2009. VisANT 3.5: multi-scale network visualization, analysis and inference based on the gene ontology. Nucleic Acids Res. 37:115–121.

Lambert, I. H., D. M. Kristensen, J. B. Holm, and O. H. Mortensen. 2015. Physiological role of taurine from organism to organelle. Acta Physiol. 213:191–212.

Lau, S. K., C. W. Lam, S. O. Curreem, K. C. Lee, C. C. Lau, W. N. Chow, A. H. Ngan, K. K. To, J. F. Chan, I. F. Hung, W. C. Yam, K. Y. Yuen, and P. C. Woo. 2015. Identification of specific metabolites in culture supernatant of mycobacterium tuberculosis using metabolomics: exploration of potential biomarkers. Emerg. Microbes Infect. 4:1–10.

Li, X. W., H. Y. Gao, and J. Liu. 2017. The role of taurine in improving neural stem cells proliferation and differentiation. Nutr. Neurosci. 20:409–415.

Lin, H., H. F. Zhang, R. Du, X. H. Gu, Z. Y. Zhang, J. Buyse, and E. Decuypere. 2005. Thermoregulation responses of broiler chickens to humidity at different ambient temperatures. II. Four weeks of age. Poult. Sci. 84:1173–1178.

Ma, X. L., L. Meng, X. X. Li, L. L. Li, Y. Wang, and X. M. Mao. 2014. Urine metabonomics study on diabetes patients by UPLC/Q-TOF MS. J. Instrum. Anal. 33:621–627.

Masaki, T., H. Yoshimatsu, and T. Sakata. 2000. Expression of rat uncoupling protein family mRNA levels by chronic treatment with thyroid hormone. Int. J. Obes. Relat. Metab. Disord. 24:162–164.

Milligan, J. L., and P. N. Winn. 1964. The influence of temperature and humidity on broiler performance in environmental chambers. Poult. Sci. 43:817–824.

Minka, N. S., and J. O. Ayo. 2012. Assessment of thermal load on transported goats administered with ascorbic acid during the hot-dry conditions. Int. J. Biometeorol. 56:333–341.

Misson, B. H. 1976. The effects of temperature and relative humidity on the thermoregulatory responses of grouped and isolated neonate chicks. J. Agric. Sci. 86:34–43.

Navarro-Reig, M., J. Jaumot, A. Garcıá-Reiriz, and R. Tauler. 2015. Evaluation of changes induced in rice metabolome by Cd and Cu exposure using LC-MS with XCMS and MCR-ALS data analysis strategies. Anal. Bioanal. Chem. 407:8835–8847.

Nichelmann, M., B. Tzschentke, and A. Burmeister. 1991. Evaporative Warmeabgabe des Geflugels bei Hoher Relativer Luftfeuchtigkeit. Arch. Geflugelkd. 55:110–115.

Nicholson, J. K., J. C. Lindon, and E. Holmes. 1999. 'Metabonomics': understanding the metabolic responses of living systems to pathophysiological stimuli via multivariate statistical analysis of biological NMR spectroscopic data. Xenobiotica 29:1181–1189.

NRC. 1994. Nutrient Requirements of Poultry. 9th ed. National Academic Press, Washington, DC.

Olubodun, J. O., I. Zulkifli, A. S. Farjam, M. Hair-Bejo, and A. Kasim. 2015. Glutamine and glutamic acid supplementation enhances performance of broiler chickens under the hot and humid tropical condition. Ital. J. Anim. Sci. 14:3263.

Plumb, R. S., J. H. Granger, C. L. Stumpf, K. A. Johnson, B. W. Smith, S. Gaulitz, I. D. Wilson, and J. Castro-Perez. 2005. A rapid screening approach to metabonomics using UPLC and oa-TOF mass spectrometry: application to age, gender and diurnal variation in normal/zucker obese rats and black, white and nude mice. Analyst 130:844–849.

Ramos, A. C., G. K. Ferreira, M. Carvalho-Silva, C. B. Furlanetto, C. L. Gonçalves, G. C. Ferreira, and E. L. Streck. 2013. Acute administration of L-tyrosine alters energetic metabolism of hippocamp us and striatum of infant rats. Int. J. Dev. Neurosci. 31:303–307.

Rasmussen, D. D., B. Ishizuka, M. E. Quigley, and S. S. C. Yen. 1983. Effects of tyrosine and tryptophan ingestion on plasma

catecholamine and 3,4-Dihydroxyphenylacetic acid concentrations. J. Clin. Endocrinol. Metab. 57:760–763.
Reece, F. N., J. W. Deaton, and L. F. Kubena. 1972. Effects of high temperature and humidity on heat prostration of broiler chickens. Poult. Sci. 51:2021–2025.
Ribeiro, R. A., M. L. Bonfleur, T. M. Batista, P. C. Borck, and E. M. Carneiro. 2018. Regulation of glucose and lipid metabolism by the pancreatic and extra-pancreatic actions of taurine. Amino Acids 50:1511–1524.
Sangster, T., H. Major, R. Plumb, A. J. Wilson, and I. D. Wilson. 2006. A pragmatic and readily implemented quality control strategy for HPLC-MS and GC-Ms based metabonomic analysis. Analyst 131:1075–1078.
Schaffer, S., and H. W. Kim. 2018. Effects and mechanisms of taurine as a therapeutic agent. Biomol. Ther. 26:225–241.
Seidel, U., P. Huebbe, and G. Rimbach. 2018. Taurine: a regulator of cellular redox-homeostasis and skeletal muscle function. Mol. Nutr. Food Res. 63:e1800569.
Touma, C., N. Sachser, and E. Möstl. 2003. Effects of sex and time of day on metabolism and excretion of corticosterone in urine and feces of mice. Gen. Comp. Endocr. 130:267–278.
Tseliou, A., I. X. Tsiros, S. Lykoudis, and M. Nikolopoulou. 2010. An evaluation of three biometeorological indices for human thermal comfort in urban outdoor areas under real climatic conditions. Build. Environ. 45:1346–1352.
Van Der Greef, J., S. Martin, P. Juhasz, A. Adourian, T. Plasterer, E. R. Verheij, and R. N. McBurney. 2007. The art and practice of systems biology in medicine: mapping patterns of relationships. J. Proteome Res. 6:1540–1559.
van der Greef, J., H. van Wietmarschen, B. van Ommen, and E. Verheij. 2013. Looking back into the future: 30 years of metabolomics at TNO. Mass Spectrom. Rev. 32:399–415.
van Loon, L. J. C., W. H. M. Saris, H. Verhagen, and A. J. Wagenmakers. 2000. Plasma insulin responses after ingestion of different amino acid or protein mixtures with carbohydrate. Am. J. Clin. Nutr. 72:96–105.
Wang, H., Z. Liu, S. Wang, D. Cui, X. Zhang, Y. Liu, and Y. Zhang. 2017. UHPLC-Q-TOF/MS based plasma metabolomics reveals the metabolic perturbations by manganese exposure in rat models. Metallomics 9:192–203.
Yahav, S. 2000. Relative humidity at moderate ambient temperatures: its effect on male broiler chickens and turkeys. Bri. Poult. Sci. 41:94–100.
Yahav, S., S. Goldfeld, I. Plavnik, and S. Hurwitz. 1995. Physiological responses of chickens and turkeys to relative humidity during exposure to high ambient temperature. J. Therm. Biol. 20:245–253.
Yousaf, A., R. Shahnawaz, T. Jamil, and A. Mushtaq. 2018. Prevalence of coccidiosis in different broiler poultry farms in Potohar region (distract Rawalpindi) of Punjab- Pakistan. J. D. Vet. Anim. Res. 7:87–90.
Yousaf, A., M. S. Tabasam, A. Memon, N. Rajput, R. Shahnawaz, S. Rajpar, T. Jamil, and M. Mushtaq. 2019. Prevalence of ascaridia galli in different broiler poultry farms of potohar region of Rawalpindi-Pakistan. J. D. Vet. Anim. Res. 8:71–73.
Yu, D., C. Luo, W. Fu, and Z. Li. 2014. New thermal-responsive polymers based on alanine and (meth) acryl amides. Polym. Chem. 5:4561–4568.
Zhao, M., D. Gong, T. Gao, L. Zhang, J. Li, P. A. Lv, and F. Gao. 2018. In ovo feeding of creatine pyruvate increases the glycolysis pathway, glucose transporter gene expression, and AMPK phosphorylation in breast muscle of neonatal broilers. J. Agric. Food Chem. 66:7684–7691.
Zhou, Y., M. H. Zhang, J. H. Feng, S. S. Zhang, Q. Q. Peng, M. Li, and X. Li. 2017. Effects of relative humidity on body heat regulation and HSP70 content of hypothalamus in broiler chicken at increasing temperature. Chin. J. Anim. Nutr. 28:60–68 (in chinese).
Zhou, Y., X. M. Li, M. H. Zhang, and J. H. Feng. 2019a. Effect of relative humidity at either acute or chronic moderate temperature on growth performance and droppings' corticosterone metabolites of broilers. J. Integr. Agric. 18:152–159.
Zhou, Y., M. H. Zhang, J. H. Feng, and H. J. Diao. 2019b. Effect of relative humidity at chronic temperature on growth performance, glucose consumption, and mitochondrial ATP production of broilers. J. Integr. Agric. 18:1321–1328.